Evaluation of Soil Resources and Groundwater Exploration for Precision Agriculture in Wadi El-Madamude, East Luxor, Upper Egypt.

Adel A. Elwan[1*] and Mostafa S. M. Barseem[2]

[1]Pedology Department, Desert Research Center, 1st Mathaf El-Matariya, 11753, Cairo, Egypt

[2]Geophysical Exploration Department, Desert Research Center, 1st Mathaf El-Matariya, 11753, Cairo, Egypt

DOI: 10.21608/AJSWS.2023.221813.1011

Article Information

Received: September 3th 2023

Revised: September 18 2023

Accepted: : September 25 2023

Published: January 1st 2024

ABSTRACT: To boost agricultural production, decision-makers must learn which crops are ideal for certain land types based on soil, water, and environmental variables. The research was carried out in the 150000 Faddan (≈ 630.3 km^2) at Wadi El-Madamude, east Luxor, Upper Egypt, to properly evaluate the water and soil resources to select the best crop for the soil type. Accordingly, a qualitative desert land potentiality evaluation (Q_LDLPE) was combined with a qualitative desert land aptness for crops (Q_LDLAC) to find the best crop for each soil type. Four landforms were researched in Wadi El-Madamude: old Nile terraces, Bajada Plain, midland, and upland. Groundwater across Wadi El-Madamude was assessed for its quality through geophysical studies. The research region of Wadi El-Madamude relies on the River Nile surface and groundwater for irrigation. Wadi El-Madamude has two groundwater aquifers: the shallow Quaternary Aquifer and the deeper Plio-Pleistocene Aquifer. High-quality River Nile water in the research region has a salinity of 175 mg/l. Groundwater salinity begins at 449 mg/l in the east and reaches 1518 mg/l near the Nile, originating from the Quaternary Aquifer. Salinity and rising water table hurt old Nile terraces due to improper irrigation and high salinity groundwater in the thick silty clay unit. Four mapping units were mapped over Wadi El-Madamude based on soil and terrain features. The analyzed Wadi lands were categorized into three categories based on Q_LDLPE methodologies: high (30%), moderate (38%), and low potential land (32%). These classes were re-evaluated for different agricultural land utilization types (LUTs) based on soil type and meteorological data using the Q_LDLAC technique. Most climate-smart crops and fruit trees were recommended for high-potential lands (45000 Faddan) on the Bajada Plain as the first priority for agricultural activity. In contrast, moderate potential lands were divided into two LUTs: 39000 Faddan on old Nile terraces for salt-tolerant crops and trees for second priority and 18000 Faddan on midland for only moderately deep-rooted crops for third priority. Low potential areas were excluded from agricultural development as non-agricultural lands due to severe restrictions such as flash flooding, soil erosion, shallowness, and low fertility. The old Nile terraces were damaged by rising water tables and increased soil salinity due to elevated groundwater caused by flood irrigation of recently reclaimed regions. Sustainable management in Wadi El-Madamude advised covering the soil with crops or plants to generate high returns with minimal inputs. It was determined and suggested that the priority order for agricultural expansion in Wadi El-Madamude should be based on the value added by climate-smart crops. The qualitative land evaluation approaches recommended precision agrarian management and climate-smart crops to enhance soil and water qualities in Wadi El-Madamude's midland soils and lower increasing water tables in its lowland soils. For future model improvement, socioeconomic data in quantity measures based on costs and profit ratios for each soil type is recommended. These models, which can be applied in various agricultural businesses worldwide, are recommended to be called Quantitative Desert Land Aptness for Crops (Q_NDLAC) and Quantitative Desert Land Potentiality Evaluation (Q_NDLPE) in order to achieve food security.

Keywords: Q_LDLPE, Q_LDLAC, Geophysical studies, Water, Soil, Crop selection.

INTRODUCTION

Over 100 million Egyptians reside on the Nile and Delta's periphery, covering less than 5% of Egypt's overall territory (≈ 1.1 million km^2) (El-Shater et al., 2021). Egypt developed a national strategy to explore groundwater and reclaim land beyond the Nile Valley and Delta to address the issue. This strategy identifies and evaluates arid land and groundwater resources to provide water sustainability for agriculture and development (Salman et al., 2019). One prospective place for this national strategy is Wadi El-Madamude in eastern Luxor, southern Egypt (Fig. 1). While groundwater study has been extensively studied, soil resources in this Wadi have not been previously explored, highlighting the urgent need for more research. Additionally, environmental impacts such as soil salinization and rising groundwater levels were seen in this Wadi (Ahmed and Fogg, 2014).

Precision agriculture is based on the availability of precise data on water, soil, climate, socioeconomic measures, and political criteria for risk mitigation, crop yield, sustainability, soil health, and food security (Walter et al., 2017; Elwan, 2019; Virk et al., 2020; Akhter and Sofi, 2022; Bhat et al., 2023). With Egypt's population growing, there is a need to considerably boost food production to guarantee Egyptians have access to nutritious food while maintaining natural desert ecosystems through intelligent and sustainable agriculture (Elwan, 2019). It is critical to match land and water resources effectively and rationally to implement precision agriculture, meet societal demands, protect desert ecosystems, and ensure sustainable crop production (Shrestha and Mahat, 2022). Land aptness and suitability evaluation determines a farmland's suitability for a specific crop cultivation practice based on correct water and soil resource data (Elwan, 2019; Bhat et al., 2023). While specific evaluation methods have been applied in developing countries, they do not always consider local realities (Swaminathan et al., 2023). Despite several shortcomings, the Storie index rating, soil irrigability classification, USDA land capability classification, and the FAO land evaluation framework continue to be the most popular guides for land evaluation methods (Elwan, 2013; Mondal and Sarkar, 2021; Fadhilla et al., 2022). As a result, Elwan (2013; 2019) established four new methods in India for land appraisal, precision farming, and sustainable planning development of desert areas, where they evolved as the world's first attempts to address the limitations of other systems. Under technological intervention, they are based on soil, water, environment, climate, socioeconomic, and political measurements concerning optimal and sustainable land use. These innovative approaches are (i) qualitative desert soil potentiality evaluation (Q_LDSPE) to determine the desert soil potential and its performance, (ii) qualitative desert land potentiality evaluation (Q_LDLPE) to assess the actual potentiality function of desert lands, (iii) qualitative desert land aptness for crops (Q_LDLAC) to suggest the land utilization types to be suited in the desert ecosystem conditions, and (iv) integrated desert land use planning (IDLUP) which is a decision-making tool to decide the best priority use for land based on the land utilization options.

Climate-smart crops and management can improve soil health, increase crop production, and mitigate climate change impacts (Akhter and Sofi, 2022; Zhao et al., 2023). These crops can be suggested as an optimal management practice in Wadi El-Madamude by following the Q_LDLPE and Q_LDLAC methods. The agricultural land potentiality evaluation using Q_LDLPE is critical in identifying lands best suited for specific crops, ensuring environmental sustainability, and maximizing land productivity. The Quantitative Land Evaluation for Crop Selection (Q_LDLAC) model is essential for understanding crop selection and predicting climate change impacts on crops.

Using technology in agriculture offers various advantages in assessing land and water parameters and gathering accurate data over broad areas (Fadhilla et al., 2022). It is also vital to understand and monitor the variations in soil and water quality within an agricultural field (Bhat et al., 2023). Soil and irrigation sensors in smart agriculture collect and control soil parameters effectively and timely (Bhat et al., 2023). Applying geographic information systems (GIS) in conjunction with Q_LDLPE and Q_LDLAC techniques has opened up new avenues for tackling site suitability evaluation difficulties. Accurate data on soil surveys and water resources in the reclaimed area are critical for crop selection and the application of precision agriculture technology to detect plant pests, reduce agrochemicals and fertilizers, predict yields, and safe water with increased harvest quality (Chapagain et al., 2022; Bhat et al., 2023).

Geophysical methods offer great potential for agricultural use. Agricultural geophysics is a subset of geophysics that focuses entirely on agricultural applications (Kayode et al., 2018). The geophysics subdiscipline may be called "agrigeophysics" as it obtains acceptance. Geophysical technologies have various agricultural uses, including precision agriculture and environmental studies. Geophysical techniques used in precision farming include electrical resistivity (ER), ground-penetrating radar (GPR), time domain reflectometry, capacitance probes, microwaves, near-surface seismic reflection, electromagnetic induction, neutron thermalization, gamma ray attenuation, and nuclear magnetic resonance (Rabeh et al., 2017). Exploration of groundwater using advances in geophysical imaging techniques in such places has grown dramatically in recent years to examine underlying geological formations over large areas (Ismail et al., 2005; Rabeh et al., 2017). Geoelectrical techniques were used to investigate groundwater conditions in the current study work. Exploring groundwater potential within the mapped structure of Wadi El-Madamude is simple once the structural setting of the area is mapped. A collection of geochemical tests of water samples collected from various water wells in the area can also be used to determine groundwater quality (Kayode et al., 2018).

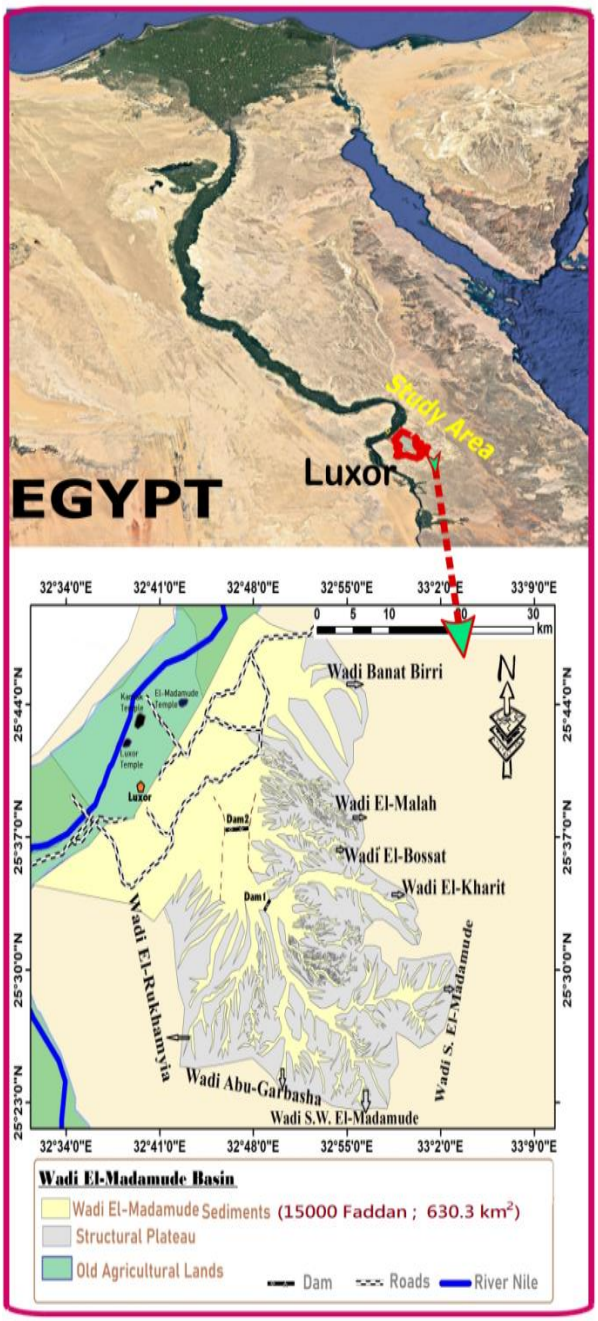

Fig. (1): Wadi El-Madamude study area location.

The current study aims to analyze groundwater using multiple references obtained through geophysical studies and to estimate groundwater quality by collecting groundwater samples from the existing wells in the studied area. Additionally, soil survey-based geospatial technology studied precise and detailed soil characteristics. The groundwater data are combined with soil characteristics and other environmental criteria to properly evaluate the land and water resources of Wadi El-Madamude to investigate the impact of groundwater and flood irrigation on the deterioration of land in Wadi El-Madamude's lowland, East Luxor, Egypt. Even though there have been numerous studies on groundwater in Wadi El-Madamude, this is the first study on Wadi El-Madamude soils for suitability evaluations, crop proposal selection, and precision farming implementation. This Wadi has enormous consequences for food security and sustainable agriculture since it allows them to provide and choose the optimum crop for their soil type, irrigation water quality, and climate circumstances.

STUDY AREA DESCRIPTION

Luxor was previously a city within the Qena Governorate before being administratively separated and renamed the "Luxor Governorate" in December 2009. The Wadi El-Madamude research area, which comprises 150000 Faddan (≈ 630.3 km^2), is located in the southern Luxor province of Upper Egypt, on the eastern side of the Nile Valley. The area is situated between latitudes 25° 23' & 25° 57'N and longitudes 32° 30' & 33° 3'E (Fig. 1), between the Nile flood plain to the west and the limestone plateau to the east.

GEOMORPHOLOGY

The DEM and landforms of the study area are visualized in Figs. 2 (Ahmed and Fogg, 2014) and 3. From west to east, the study area is distinguished by the presence of the following geomorphologic units: the old Nile terraces and Bajada Plain as lowland, the midland of Wadi El-Madamude and the hydrographic system including Wadi El-Madamude tributaries as upland, and the structural plateau (Fig. 3). The old Nile terraces occupied mainly by the cultivation and reclamation processes and it is developed into successive terraces rising to 65 m above the present level of the floodplain. It is underlain by silty clay deposits resulting from the consecutive floods of the present Nile. The surface of this plain is nearly flat, slopes very gently northward, and has an elevation ranging from 71 to 96 m above sea level. A complicated irrigation system of canals and drains incises this plain's surface. The nearby alluvial flats of Wadi El-Madamude and its tributaries are included in the Bajada Plain. It is formed of a mixture of sand and gravel. The drainage system's complex dry streams are cut into these terraces and continue to the low areas of the young alluvial plain. The eastern structural plateau has a one-of-a-kind setting, forming a separate dissected plateau with its hydrographic system (Fig. 3).

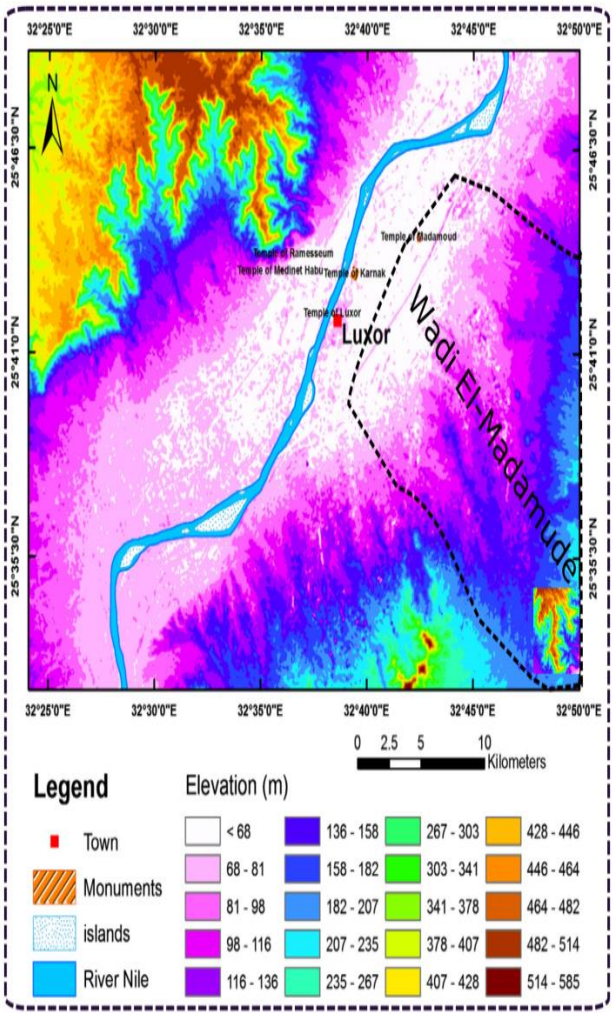

Fig. (2): DEM map showing the elevations of a significant part of the Wadi El-Madamude study area (after Ahmed and Fogg, 2014).

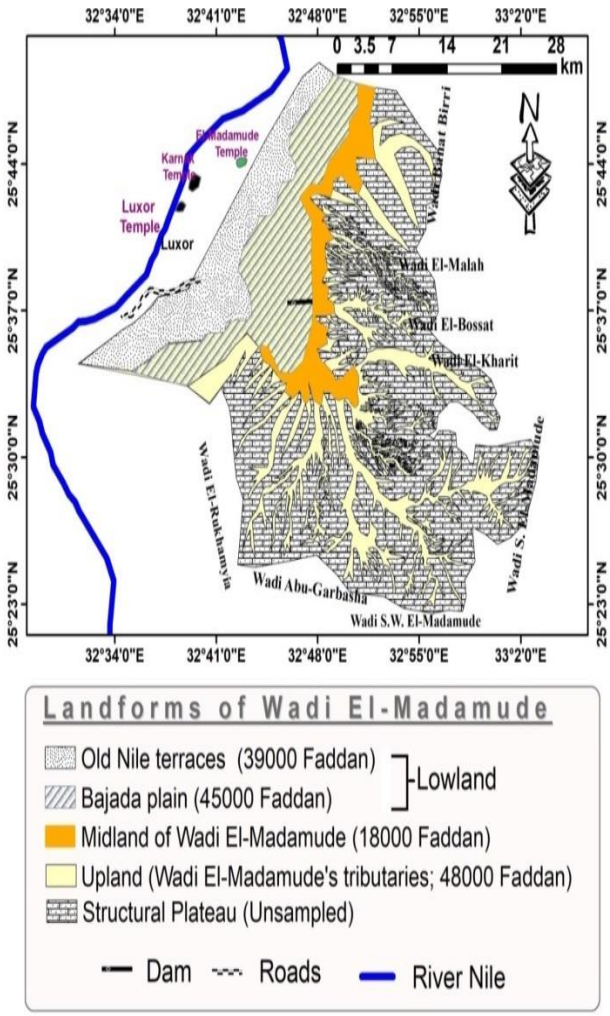

Fig. (3): Geomorphological units of Wadi El-Madamude study area (1 Faddan ≈ 4200 m^2).

GEOLOGIC SETTING

Said (1990) and Kamel (2004) investigated the surface geology of the study area (Fig. 4). The Arken Formation's Holocene deposits were formed by the silty clay strata ejected by the Neonile. The sediments of Prenile created enormous cross-bedded river sands interbedded with clay lenses (Qena Sand) throughout the Middle-Late Pleistocene. Conglomerates deposited throughout the middle Pleistocene to form the Abbassia Formation and Qena Sand. The armant formation is a Plio-Pleistocene (Protonile-Prenile) deposit composed mostly of clays, sands, and conglomerates. The Paleonile Pliocene Sediments' El-Madamude formation was created from brown clays interbedded with thin, fine-grained sand and silt laminae. Tarawan Chalk's carbonate unit is on top of the Dakhla Shale. Dakhla shale comprises dark grey papery shale and marl with interbedded siltstone, sandstone, and limestone. Esna Shale is made up of laminated green and grey shale. The Thebes Formation was composed of limestone with flint bands. Quseir Shale comprises thin-bedded, highly variable color shale, siltstone, and sandstone. The Duwi Formation comprises alternating claystone beds, sandstone, siltstone, and oyster limestone. The Dakhla Shale is an Upper Cretaceous deposit.

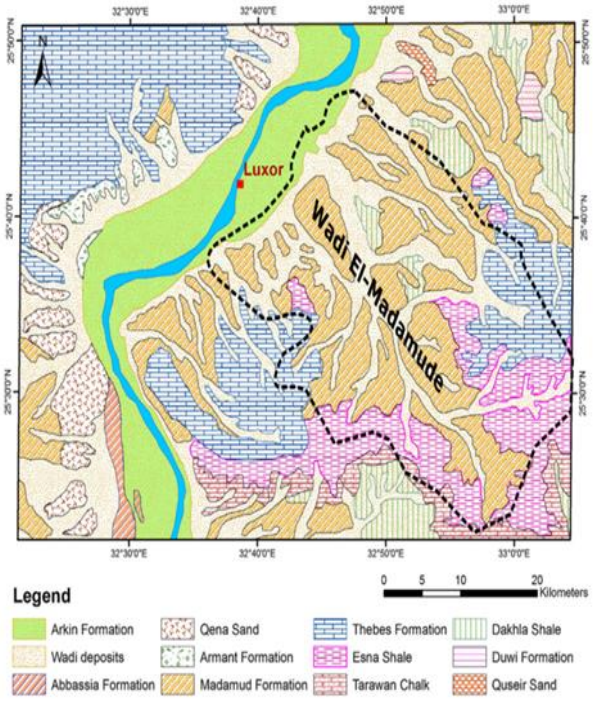

Fig. (4): Surface geological formations on lands of Wadi El-Madamude study area (compiled from Kamel, 2004; Ahmed and Fogg, 2014).

The stratigraphic units in the Wadi El-Madamude research region have been identified using Dupuis et al. (2003) 's latest stratigraphic examination (Figs. 4 and 5). The Lower Eocene Thebes Limestone Formation, Late Maastrichtian to Middle Paleocene Dakhla Shale Formation, Landanian-Late Paleocene Tarawan Chalk Formation, and Upper Paleocene-Lower Eocene Esna Shale Formation are the units. The research region is in the Nile Valley's eastern outskirts, bordered by Eocene-age limestone elevated structural plateau and underlain by Paleocene-age shale (Fig. 5). The research area's old Nile terraces and alluvial plains slope gradually to the north and east.

CLIMATE AND HYDROLOGY

Wadi El-Madamude's climate varies throughout the year and is characterized by desert and arid conditions (Egyptian Meteorological Authority, 2022). The maximum air temperature in July is 49.9°C, while the minimum is 22.7°C in January. The monthly average relative humidity (RH) in May and December was 25-55%. The monthly average wind speed in October was 5.9 km/h (maximum), whereas in April, it was 9.3 km/h (minimum). Precipitation in Wadi El-Madamude occurs at random throughout the year. It may be insignificant (Ahmed and Fogg, 2014) (Fig. 6). The Wadi El-Madamude morphometric analysis is of high hazard degree 5 for flash flooding. The total volume of water flow that reaches its Delta (Bajada Plain) is projected to be 592 million cubic meters (El Shamy et al., 2013).

These are younger, densely cultivated plains coated in Holocene silt and clay. Pleistocene sand and gravel fill the recovered area (Kamel, 2004) (Fig. 4). The Wadi El-Madamude sedimentary sequence is as follows: Arkin Formation, Modern River Nile sediment of Holocene sediments, and Armant Formation, Qena Sand and Abassia Formation, Wadi deposits of Pleistocene sediments. These sediments are part of the Quaternary rock units. Lower Eocene-Palaeocene sediments (Thebes Formation, Esna Shale, Tarawan Chalk) and Pliocene sediments (El-Madamude Formation) comprise the Tertiary Rock Units (Fig. 5) (Ismail et al., 2005; Ahmed, 2009).

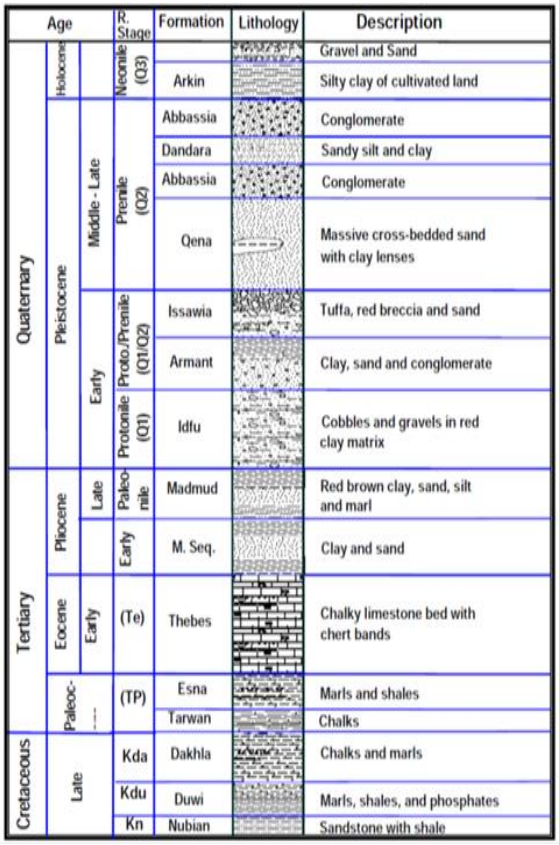

Fig. (5): Composite stratigraphic column for Wadi El-Madamude study area (after Ismail et al., 2005; Ahmed, 2009).

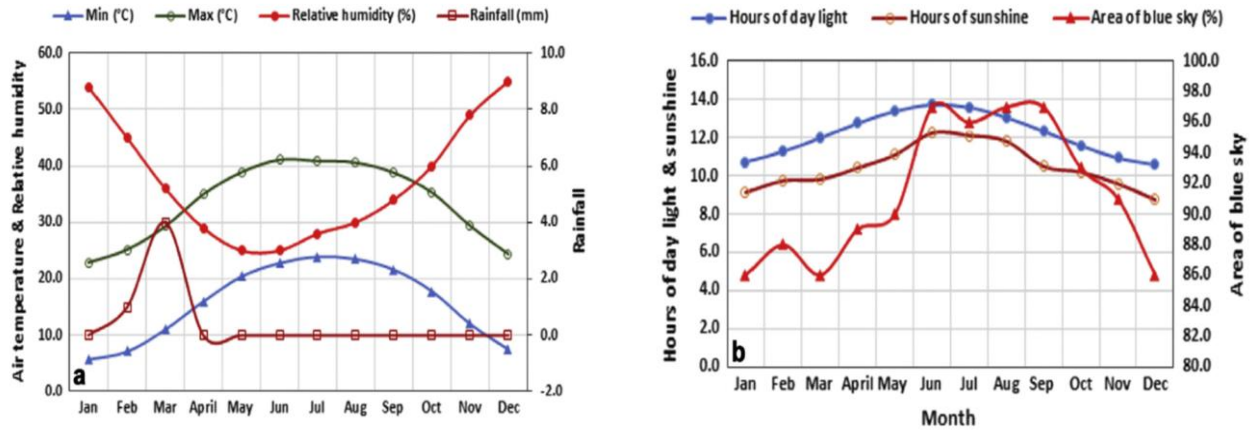

Fig. (6): Climate conditions of Wadi El-Madamude study area. a) rainfall and relative humidity, b) hours of blue sky area, sunshine, and day light (illustrated in Ahmed and Fogg, 2014).

The research region's irrigation sources are the Nile's surface and groundwater. Salman et al. (2019) identified two groundwater aquifers in Wadi El-Madamude: the shallow Quaternary Aquifer and the deeper Plio-Pleistocene Aquifer (Fig. 7). Quaternary Aquifer, with a local thickness of 5-95 m, consists of graded gravel, sand, and some clay. This aquifer is semi-contained by higher silty clay in the central Nile Valley. The silty clay layer thins and ends at the river valley's outskirts in the phreatic aquifer. The regional groundwater flows east-west towards the Nile Canal (Ahmed 2009). Ahmed et al. (2014) identified the Plio-

Pleistocene Aquifer as the secondary aquifer in the research area, consisting of gravel, sand, and clay (Fig. 7). This aquifer is seen at Nile Valley's rim. The salinity of the Plio-Pleistocene Aquifer is substantially higher than the Quaternary Aquifer (Ahmed, 2009). El Shamy et al. (2013) found that a series of normal faults affected the hydrogeologic setting of the research region, creating a graben-like feature in the valley (Fig. 7). Because of this faulting, different hydraulic qualities of groundwater aquifers have been distributed. The Quaternary aquifer, which forms the old cultivated areas on both river banks, encompasses the Nile Valley's center strip and is the most essential water-bearing deposit in the studied region. This aquifer comprises the higher Holocene aquitard and the lower Pleistocene aquifer (Ahmed and Fogg, 2014;Salman et al., 2019).

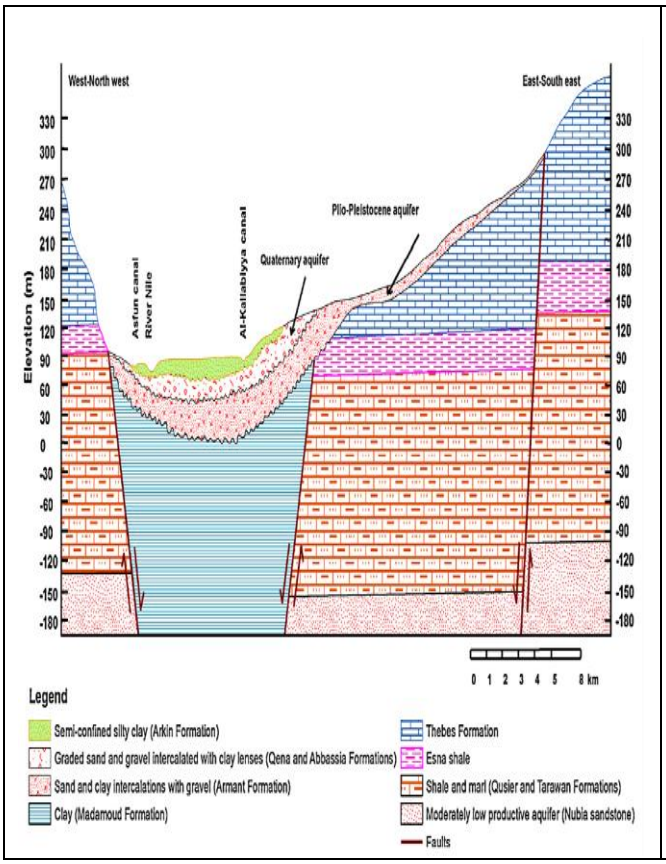

Fig. (7): Hydrostratigraphic section representing the Wadi El-Madamude study area (Kamel, 2004; Ahmed and Fogg, 2014; Salman et al., 2019).

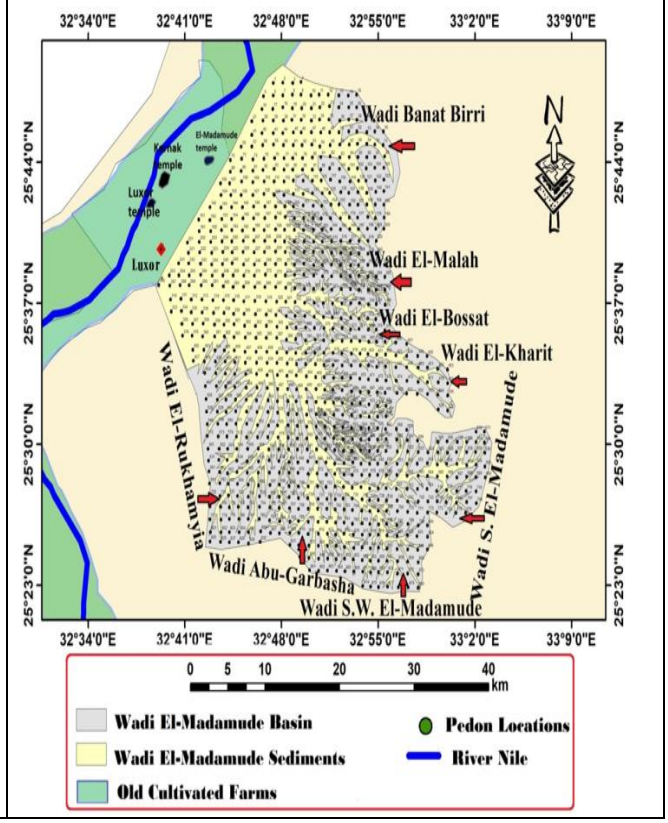

Fig. (8): Soil pedons location grid across the Wadi El-Madamude study area.

MATERIALS AND METHODS

Fieldwork

A pedon grid soil survey was conducted on all the Wadi El-Madamude landscapes and landforms. Four landforms were identified and sampled. These are old Nile terraces, Bajada Plain, midland, and highland tributaries of Wadi El-Madamude (Fig. 3). Soil pedon pits were opened at representative landforms to conduct soil characterization. The soil pedons were studied to a depth of >200 cm, and their morphological properties were reported in situ based on Schoeneberger et al. (2012) and FAO (2006a). Soil color charts were used to define the soil color (Munsell Color, 2009). Water samples were collected from different wells across study area (Fig. 9). For soil and water laboratory studies, standard laboratory techniques were used.

The resistivity value decreases when the rock contains clays, as numerous authors have observed in their investigations (Reynolds, 2011; Othman et al., 2019). Based on the interpretation results of "40" one-dimensional vertical electrical sounding (1D VES) at various locations in Wadi El-Madamude, Ismail et al. (2005) studied the Quaternary aquifer water to fully comprehend the underlying structures and groundwater condition in comparison to groundwater data of Plio-Pleistocene aquifer studied by Youssef (2020). Several vertical electrical soundings (VESes) were performed between 700 and 1000 m with maximum current electrode spacing AB/2 (Youssef, 2020). Geophysical techniques, particularly geo-electric ones, were successfully used to detect aquifers' new-water/saltwater interface. Resistivity overviews are widely employed to search for groundwater in permeable and fissured substrates (Youssef, 2020). The technique provides precise information on the geometry, source, and overall pollution level. As a result of these factors, geoelectrical display research is constructed by Ismail et al. (2005) and Youssef (2020) to investigate and assess the hydrogeological management in the study region.

The study of Youssef (2020) uses the VES method to subdivide the shallow portion into strata with varied lithologies and water contents in the subsurface of Wadi El-Madamude. In this study, 31 VESes are performed by Youssef (2020) using a Schlumberger array to explore the vertical distribution of the studied resistivity layers. The geographical and geologic

features of the site govern the spacing between VES stations. The field resistivity curves were created by Youssef (2020) by plotting the apparent resistivity data on log-log graph paper. When the findings of geoelectrical data interpretation are displayed in contour maps, they can better depict the subsurface structure of the area. The lateral variation of a particular horizon's characteristic (depth, resistivity, etc.) is characterized by Youssef (2020) throughout the researched region. When the findings of the geoelectrical data interpretation are displayed as contour maps, the underlying structure of the area may be more precisely depicted (Youssef, 2020). The maximum current electrode separation ranged from 0.6 to 1 km, and the distance between neighboring sounding centers ranged from 1 to 3 km (Ismail et al., 2005). Resistivity data was evaluated to identify geo-electric units in the research region. Next, interpretations were used to create geo-electric resistivity cross-sections, subsurface resistivity, and thickness maps. The geologic/hydrologic units in the research region's shallow subsurface (100m) were characterized by Ismail et al. (2005).

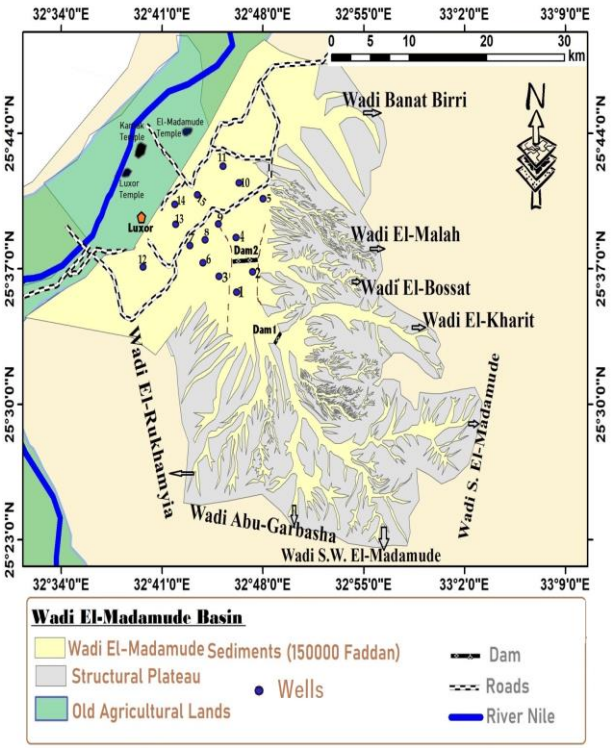

Fig. (9): The groundwater samples location collected from different wells across Wadi El-Madamude of Upper Egypt.

Laboratory Analyses

Soil physical, chemical, and fertility properties were measured per the standard soil analysis procedures adopted by Mani et al. (2007) and Soil Survey Staff (2014). The core sampling method was utilized for bulk density measurement (Lu, 2000). Available Nitrogen (AK) was determined as per the standard procedures of FAO (1970). Fe, Zn, Cu, and Mn micronutrients were determined using the diethylenetriaminepentaacetic acid (DTPA) methods (Lindsay and Norvell, 1978). Surface and groundwater samples were evaluated using standard protocols and methodologies of Mani et al. (2007).

Chemical analysis was performed on the collected Nile surface water samples (Fig. 9). In Wadi El-Madamude, 15 groundwater samples were obtained using hand pumps or existing wells for chemical analysis. The investigated wells are from the Quaternary Aquifer (Fig. 9). The temperature was checked during pumping to ensure that stagnant water was removed from the well hand pumps. The EC_w (dS/m), total dissolved salts (TDS; mg/l), cations, and anions were estimated.

Land Evaluation Procedures

In 2013, the Q_LDLPE and Q_LDLAC models were established for the first time in India to evaluate desert ecosystem resources, specifically for hyperarid, arid, and semi-dry zones (Elwan, 2013; 2019). A potentiality index is calculated using twenty-two parameters, including the environment, soil pedon, socioeconomic measurements, human management, markets, political entity, and climate conditions. Each parameter is assigned a numerical weight and a rating value. Elwan (2013; 2019) provides the numerical rating values of criteria and their weights. Water availability, natural risks, and topography are all environmental requirements. The soil pedon criteria include effective soil depth, coarse fragments and surface stoniness, soil texture, available soil water, natural drainage, pH, gypsum, CaCO3, ECe, fertility status, and soil color. Furthermore, the socioeconomic state comprises labor availability, infrastructure, human management, markets, and precision farming technologies. On the other hand, agricultural policies, decision-making, and land tenure constitute the political entity. The following index is positioned to a potentiality category of soil and land. The potential types are as follows: (i) high potential land has a resultant index of 81-100%, (ii) moderate potential land has a resultant index of 66-80%, (iii) mild potential land has a resultant index of 46-65%, (vi) low potential land has a resultant index of 26-45%, and (v) non-potential land has a resultant index of less than 25%. The following is how the index is calculated: Q_LDLPE (%)= $\sum(\boldsymbol{R_c \times W_c})$; Where R_c is the rating score of each of the 22 criteria, and W_c is the weighting score of the 22 criteria related to water, soil, socioeconomic measures, and political entity.

Methodologies of land suitability and crop priorities followed in the present study are given in Fig. 10. Q_LDLAC is a specialized approach for recommending different crops for desert land evaluation and management based on precision farming. It also empowers people to decide how to allocate desert land resources (Elwan, 2013; 2019). Q_LDLAC rules were modified based on specific soil parameters, environmental risks, and climate needs for plant growth to adapt to the local conditions in Egypt (Elwan et al., 2016; Elwan, 2020).

The Q_LDLAC model is based on a comparison of plant requirements with available land and water. It involves matching crop growth requirements with twenty-seven criteria of the environment, soil, socioeconomic measures, political entity, and climate (Fig. 10). Q_LDLAC takes into account the twenty-two

criteria of the Q_LDLPE model, as well as the five climate parameters (temperature, evapotranspiration, relative humidity, wind velocity, and precipitation). The land aptness process includes the following steps: (i) Q_LDLPE identification and determination of land potentiality; (ii) crop requirements; (iii) matching process of the previous two; (iv) screening the land aptness options into land use recommendation; and (v) defining of aptness class and crop selection process. The following rules determine the final land aptness class: (i) If one or more of the criteria, such as climate, irrigation water availability, and soil depth, is/are limiting, then the worst case is the final class; and (ii) For all other criteria, if the worst case is fulfilled in three or more criteria, then this is the final land aptness class. The matching procedure and the weight of limits differentiate four aptness classes (high, moderate, slight, and non-aptness). The soils under study were assessed for suitability for producing various crops using the crop growth requirements described by Naidu et al. (2006). Elwan (2013) provided the criteria and procedures for assigning aptness classes to land.

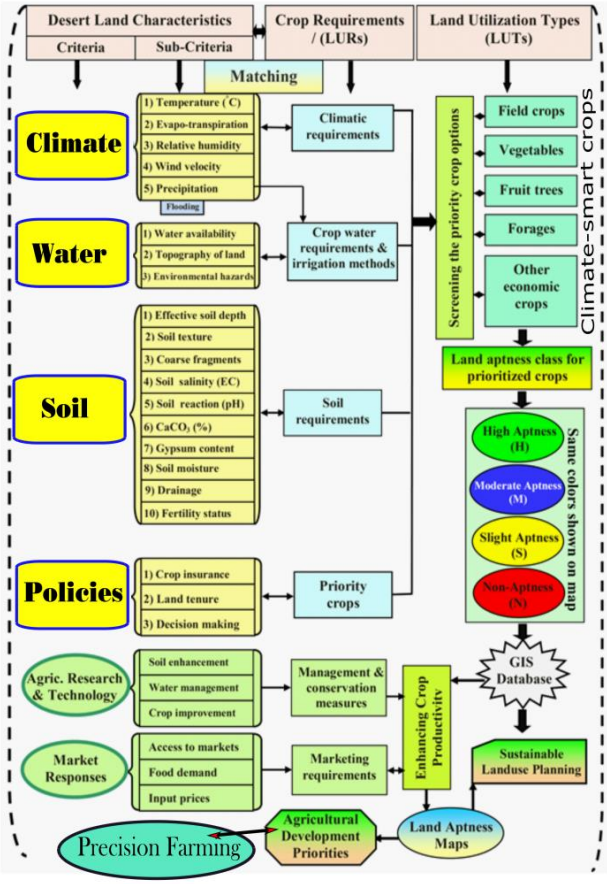

Fig. (10): Flowchart of the qualitative evaluation of desert land aptness for crops (Q_LDLAC) (modified after Elwan et al., 2016; Elwan, 2019).

The socioeconomic indicators in Wadi El-Madamude such as infrastructure of roads, labor, agricultural technologies, human management, and markets, as well as political entities (e.g., decision-making, agricultural policies, and land tenure), were collected using field surveys with local people and statistics data of Luxor (Central Agency for Public Mobilization and Statistics of Egypt, 2022).

Data Processing and Statistical Analyses

ArcGIS 10.1 software (ESRI, The Redlands, CA, USA) was used to identify the locations from which the pedons were collected to develop thematic maps of landforms, soil mapping units, and land appraisal potentiality, as demonstrated in this work as figures. All statistical analyses (e.g., mean and standard deviation) were performed for the soil data using the Statistical Package for the Social Sciences (SPSS) software (IBM® SPSS® Statistics).

INTERPRETATION OF RESULTS

Soil Mapping of Wadi El-Madamude

Across the Wadi El-Madamude research region, four soil mapping units were defined based on effective soil depth, soil texture, soil salinity, $CaCO_3$ content, and land topography (Fig. 11). SMU1 stands for moderately fine textured, moderately saline, strongly calcareous soils with almost flat topography (Figs. 11, 12, and 13). In contrast, SMU2 stands for deep, moderately coarse textured, slightly saline, strongly calcareous soils with gently undulating topography (Figs. 11 and 14). SMU3 stands for moderately deep, coarse-textured, slightly saline, moderately calcareous soils with undulating topography, while SMU4 stands for shallow, coarse-textured, nonsaline, slightly calcareous, with undulating topography (Fig. 11).

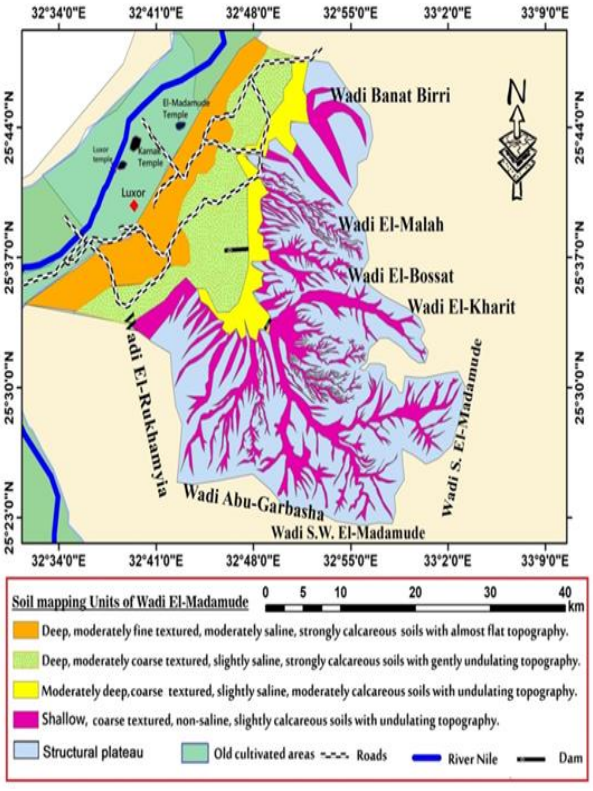

Fig. (11): Soil mapping units across Wadi El-Madamude study area.

The Wadi under consideration has three land positions: upland, midland, and lowland. Wadi El-Madamude tributaries (upland) include Wadi Banat Birri, Wadi El-Malah, Wadi El-Bossat, Wadi El-Kharit, Wadi South El-Madamude, Wadi S.W. El-Madamude, Wadi Abu-Garbasha, and Wadi El-Rukhamyia (Fig.

11). midland is regarded as the principal channel of Wadi El-Madamude. The lowlands cover 84000 Faddan (56% of the sampled area) and are divided into two landforms: old Nile terraces tested by SMU1 and Bajada Plain sampled by SMU2 (Table 1). SMU3 depicts the midland, whereas SMU4 represents the upland.SMU1 covers 39000 Faddan (26% of the sampled area), while SMU2 covers 45000 Faddan (30%). SMU3 has a land area of 18000 Faddan (12%), while SMU4 has a total of 48000 Faddan (32%).

SMU1 soils on old Nile terraces are typically planted with various crops yearly (Figs. 11 and 12). Sugar cane, fruit trees, orchards, date palms, and alfalfa are permanent crops, whereas clover, wheat tomatoes, dry beans, garlic, vegetables, barley, melons, and fenugreek are winter crops. Maize, sesame, peanuts, roselle, sorghum, soybeans, tomatoes, and other crops are grown in the summer and Nili. Mismanagement reigns supreme in this area, where flood surface irrigation was primarily employed for irrigation (Fig. 12). Rising water tables and increased soil salinity have damaged soil and groundwater properties and reduced crop productivity. Changes in groundwater levels correspond to changes in agriculture, which may contribute to increased salt in groundwater (Ahmed and Fogg, 2014).

Flood irrigation practices mismanagement (Fig. 12a,b), together with the climatic (Fig. 6) and hydrologic circumstances of Wadi El- Madamude's lowland, enhanced weathering processes that contributed to the deterioration of these resources (Fig. 12c). Before the construction of the High Dam, groundwater levels in the Nile Valley fluctuated depending on the Nile's water level. In the summer, the groundwater level was too deep to allow salt production on the soil surface via evaporation and capillary action (Fig. 12c). Furthermore, with the seasonal flood gone and significant year-round irrigation (Fig. 12b), groundwater levels remained consistently high, resulting in waterlogging and capillary action (Figs. 12c & 13). Soil salinity rose as the distance between the surface and the groundwater table was small enough to raise salts on the soil surface (Fig. 12c), degrading soil characteristics and reducing crop production (Fig. 12d).

Soil Morphological Characteristics

Table 1 shows the pedomorphological characteristics of Wadi El-Madamude. Field observations revealed that some SMU1 land had deteriorated due to soil salinization, salt crystallization in walls and columns, capillary groundwater seepage, and discoloration (Fig. 12; Table 1). According to FAO (2006a), all the pedons of SMU1 were very deep (>150 cm) with almost flat topography (Fig. 13). The adequate soil depth that does not impede root growth governs the amount of water and nutrients available to plant roots (Bhat et al., 2023). The field study revealed that the lower topsoil and subsoil horizon boundaries in SMU1 pedons were gradually and smooth. SMU1's soil wet color was brown (7.5YR 4/2) over all surface horizons, but the other SMUs' surface layers ranged from yellow (10YR 8/6) to very pale brown (10YR 8/2; 8/4) (Figs. 13 and 14). The color of the subsurface soil ranged from very dark grey (10YR 3/1) in SMU1's Btkz and Btkm horizons to brown (7.5YR 4/4) in SMU2's Bk calcic horizon (Fig. 14; Table 1). The Btkm and Btm horizons are tough layers that imply relatively well-drained soil due to the deposition of lime and clay (Fig. 13; Table 1). The variance in color between pedons and vertically within a pedon layer is most likely owing to variations in iron oxide and lime forms, parent material types, OM concentration, and drainage conditions.

SMU1's topsoil structure was granular in the Ap horizon, transitioning in the subsoil from subangular blocky to enormous structureless. In the subsoil, the granular soil structure of SMU1 was replaced by angular and subangular structures. Granular soil structures are created when the surface horizons have higher OC levels (0.45%). Blocky structures form in the subsurface horizon due to the underlying layers, a decrease in soil organic matter, a higher clay content, and a decrease in plant roots. SMU1's surface and subsurface horizons' dry consistency ranged from soft in the Ap horizon to very hard in the Btkz and Btkm horizons (Table 1). These very hard subsurface horizons and strata may be linked to decreased OC content, more clay particles, and lime content. Waterlogging impaired the deepest horizons (Btg) of SMU1, although soils in other SMUs were not affected by waterlogging and had an excellent natural drainage class.

Soil Physical Characteristics

Table 2 displays soil physical properties data. Hazelton and Murphy (2016) categorized soil clay, sand, and silt particle concentrations as very high (>50%), high (40-50%), moderate (25-<40%), low (10-<25%), and very low (<10). According to the ratting and weighted mean value of examined pedons, SMU1 soils had moderate sand (35.2%), silt (37.2%), and clay (27.6%) content (Table 3). The clay concentration grew somewhat within the depths of the examined pedons up to 155 cm, then dropped. Most subsurface horizons (Btkm&Btkz) are argillic or calcic, resulting from clay mineral or lime erosion from topsoil Ap layers. This observation aligns with Dinssa and Elias' (2021) discoveries that clay minerals may be inherited from parent materials through weathering or degradation of primary minerals. Clay mineral structure and weathering processes impact soil fertility and water retention (Dinssa and Elias, 2021). The particle size distribution of sand and silt in most of the examined pedons displays an uneven pattern across soil depth (Table 2). Clay films (CLF) were discovered on the sides of ped faces of Btkz and Btkm horizons (Table 1), showing that clay particles migrated downward.

The silt/clay ratio of SMU1 pedons' surface and subsurface soils ranged from 0.73 in Btkz to 2.54 in C horizon (Table 2). The clay/silt ratio did not correlate with soil type or depth in the study. Ahukaemere et al. (2017) found that soils with a silt/clay ratio below 0.15 are extensively heavily weathered, while those above 0.15 have a higher weathering potential and are younger. All tested soils showed this pattern. The soil studied in this work is still new. Hazelton and Murphy

(2016) suggest that the optimal bulk densities of mineral soils at surface horizons are 1.2-1.4 g/cm^3. SMU1 and SMU2 soils exhibit variable bulk density (BD) near the optimal range, likely due to overlay soil mass, low porosity, and decreased OM content in lower surface layers. The bulk density of surface horizons varies from 1.1 g cm^{-3} in SMU1's Ap horizon to 1.65 g cm^{-3} in SMU3's C layer. Additionally, bulk density ranges from 1.26 g cm^{-3} in SMU2's Bk horizon to 1.76 g cm^{-3} in SMU4's Cr layer (Table 2). In SMU1 and SMU2, low topsoil BD did not affect root penetration, water availability, or crop production. However, SMU3 and SMU4 soils had differing bulk densities. Conversely, SMU1's deeper horizons (Btkz and Btkm) had higher BD values, limiting rooting zone and vertical drainage class inside pedons.

According to Hazelton and Murphy (2016), soil with AWHC levels of <10%, 10–20%, and >20% were rated as low, medium, and high. The soils under examination have a weighted mean AWHC of 14.6%, making them appropriate for agricultural production. SMU1's Ap horizon has the highest AWHC (17.8%; Table 2), clay content (21.06%; Table 2), and highest OC (0.45%; Table 3), with low bulk density (1.1 g cm^{-3}; Table 2). Dinssa and Elias (2021) found that plant-available water capacity was most lacking in sand due to low specific surface area, whereas increasing silt content resulted in the highest AWHC.

Soil Chemical Characteristics

Tables 3 and 4 show the selected soil chemical and nutritional parameters of the studied pedons. According to the Soil Science Division Staff (2017), examined soil extracted by saturated paste is divided into three groups: moderately saline (5.9-15.2 dS/m) in SMU1, slightly saline (2.9-5.8 dS/m) in SMU2 and SMU3, and nonsaline (<2dS/m) in SMU4 (Table 3). This process is due to heavy base leaching from Wadi El-Madamude's upland (SMU4) to the lowland (SMU1 & SMU2). Overall, soil pH values increased modestly with depth in the first three layers of SMU1 pedons. Except for the deepest layer of SMU1 pedons, the soil pH is greater than 8 for the surface and subsurface horizons. The pH of the surface horizons in the studied soils ranged from 7.8 in the C layer of SMU3 to 8.3 in the Ap horizon of SMU1 (Table 4). The Btkz of SMU1 had the highest pH value (9.1), indicating that it was very strongly alkaline, which might be attributable to greater levels of lime (25.4%) and ESP (16.5%). Lime concentrations in SMU1 and SMU2 soils range from 8.6% in the Btm horizon of SMU1 to 26.5% in the 2Ck1 of SMU2, indicating strong calcareous soils, according to FAO (2006b). Schoeneberger et al. (2012) reported that the pH values of all pedons were within the range of somewhat alkaline to very strongly alkaline across their horizons. Some crops have a yield loss inside this fundamental pH range. It was discovered that the soils' gypsum content was modest (0.1-3.9%), indicating that they were not gypsiric soils. The reclamation of the soils using gypsum or the selection of crops is required.

a)Flood surface irrigation mismanagement b) Soil flooding and waterlogging c) Surface salinity crust and soil degradation

d) The crop grown in the incorrect soil type

Fig. (12): Failure to use precision farming techniques and choose the proper crop pattern for the soil type in the soils of SMU1.

The OC concentration of the investigated Pedons varied (Table 4). According to Hazelton and Murphy (2016), the OC concentration of topsoil and subsoil was in the 0.01- 0.45% range, with greater values recorded in surface layers. All pedons' soil OC content decreased with increasing soil depth (Table 3). According to FAO (2006b), the weighted mean CEC in SMU1 at the lowland of Wadi El-Madamude was medium (22.7 cmol (+) kg^{-1}), but in SMU1 it decreased to 16.7 cmol (+) kg^{-1} and declined to 6 and 5.2 cmol (+) kg^{-1} in SMU3 at midland and SMU4 at upland, respectively. CEC values in lowland soils were generally medium, indicating high nutrient retention and buffering capabilities, but CEC values in upland soils were low (FAO, 2006b). Because of base leaching vertically and horizontally throughout the landscape and low clay concentration, upland soils have low CEC values. The soil surface horizons had a Ca/Mg ratio of 4.61 for SMU1, 2.61 for SMU2, and 0.93 for SMU3. A low ratio in the upland suggests a low Ca value for most crops. Hazelton and Murphy (2016) found that a Ca/Mg ratio below 4:1 causes low Ca availability, meaning a possible shortage due to excess Mg or flash flooding from highland to lowland. Ca/Mg ratios were consistently lower for most pedons and unevenly distributed for others across soil depth.

The soils in the research area had low nitrogen levels (0.9 to 9.6 ppm) according to the critical limits of Hazelton and Murphy (2016). This level may be due to certain soils' low organic carbon levels. Available phosphorus levels were low in Midland soils (0.7-6.9 ppm) and low to medium in lowland soils (7.1-23.9 ppm) (Table 4). This level may be due to lime and Ca/Mg hydroxides fixing liberated phosphorus. Low potassium concentrations (3.2-47.7 ppm) were found in the examined soils. Low organic matter and nitrogen levels are typical in semi-arid soils, where rapid mineralization hinders carbon buildup. Lowland pedons have more nitrogen and organic matter content than other types. The distribution of OC in these soils is mainly linked to physiography and slope position.

The weighted mean of available nitrogen (AN) and phosphorus (AP) in SMU1 at lowland was 20.9 mg/kg and 5.6 mg/kg, respectively, indicating low levels. However, accessible potassium (AK) was moderate (115.4 mg/kg) (Table 4). The upper soil layer had higher AN levels (29.1 mg/kg) and similar patterns with OC in all pedons (Table 3), indicating a substantial link between TN and soil OC. This research confirms Dinssa and Elias' (2021) findings that OC comprises 93-97% of soil N concentration. The soil's surface layers exhibited ideal AP and AK levels for lowland agricultural crop production but low to medium in midland and highland (Table 4).In highland locations, low soil accessible P may be caused by Ca^{++} and Mg^{++} fixation in high soil pH circumstances. Phosphorus fixing is common in alkaline, dry soils. Low P and N levels significantly impact agricultural output in the studied area. This investigation confirms Dinssa and Elias (2021) findings that Ethiopian soils lack phosphorus. In all soil profiles, P declines due to decreasing OC levels and base fixation at subsurface horizons (Tables 3 and 4).

Groundwater Exploration in Wadi El-Madamude

Figs. 15, 16, 17, and 18 display the geoelectrical sections, isopach map, true resistivity of the Quaternary aquifer, and iso-salinity map in Wadi El-Madamude with the aide of Ismail et al. (2005). Initially, lithologic control from nearby boreholes was used to correlate actual resistivity curves (Figs. 15 and 17). High resistivities (~20Ω-m) were found in the upper dry silty clay, low resistivities (~4Ω-m) in the moist silty clay, and significantly higher resistivities (~50Ω-m) in the graded sand and gravel of the Quaternary Aquifer. The true resistivity curves show the fourth geo-electric unit, with low resistivity (<10Ω-m) at depths greater than boreholes. The deeper unit is likely located in the Plio-Pleistocene Aquifer (sand, clay, silt, and gravel) based on existing geological/hydrological data.

The area's geo-electric resistivity includes four to five units: dry topsoil, moist silty clay, Quaternary and Plio-Pleistocene aquifers, fine sand and silt from reclaimed land, and limestone from the eastern plateau's foot (Fig. 15). This research reviews the thickness and resistivity of four geo-electric units (Fig. 16), although only the second and third units of the Quaternary aquifer are examined by Ismail et al. (2005). The second geo-electric unit thickens near the Nile, then thins and pinches eastward (Fig. 16). Its high thickness (12-28m) under old Nile terraces suggests its deposit in a paleo-Nile meander. An abnormality of this scale must impact the local hydrologic ecosystem. This process could lead to decreased capillary water rise, lateral groundwater flow, surface water vertical drainage, and increased salinity near the paleo-meander .

Figs. 15 and 16 showed that the third geo-electric unit has considerable resistivity of 17-95Ω-m and significant thickness of 10-60m (Ismail et al., 2005). The Quaternary Aquifer in the study area is composed of sand, silt, and gravel. The geo-electric unit has a higher resistivity than the Plio-Pleistocene Aquifer's silty clay and underlying sand and clay. The resistivity contrasts determined the thickness and resistivity of the unit. Lower resistivity values are observed in the third unit near the River Nile. The drop in resistivity may be due to increased groundwater salinity in this direction or lateral lithologic changes, as confirmed by groundwater salinity data.

Hydrological Results

Table (5) displays groundwater analysis (TDS and main ion concentrations). The River Nile water in the research area has a salinity of 175 mg/l, indicating high quality. Groundwater salinity varies from 449 mg/l in Wadi El-Madamude to 1518 mg/l near the Nile, following groundwater flow from the Quaternary Aquifer (Table 5) (Fig. 18; Ismail et al., 2005). High total salinity values in Luxor may be due to 1) lack of rainwater leaching; 2) evaporation of surface water and flushing of residual high salinity water into the subsurface; 3) poor drainage in low-permeability silty clay areas; and 4) leaching of salts from nearby fields or sewage.

Table (1): The organized soil morphological data for soil mapping units at Wadi El-Madamude, East Luxor, Upper Egypt.

Horizon (cm)	Horizon suffix	Moist color	Pedogeneic features	Structure	Natural drainage	Dry consistence	Vegetation roots	Topography and flooding risk	Position and landform
SMU1: Deep, moderately fine textured, moderately saline, strongly calcareous soils with almost flat topography.									
0–15	Ap	7.5YR 4/2	CAN	Granular	Moderately well drained	Soft	Few, medium	Almost flat & low flooding risk	Lowland: Alluvial plain (Downstream)
15–45	Bw	7.5YR 5/8	CAM	Subangular blocky		Slightly hard	Common, fine		
45–70	Btkz	10YR 3/1	CAM,FDS, CLF	Angular blocky		Very hard	Very few, fine		
70–115	Btkm	7.5YR 5/8	CAN,SAX, CLF	Massive		Very hard	None		
115–155	Btm	7.5YR 4/6	CAM	Subangular blocky		Hard	None		
155-205	Btg	10YR 5/4	None	Massive		Very hard	None		
205+	W	Water table							
SMU2: Deep, moderately coarse textured, slightly saline, strongly calcareous soils with gently undulating topography.									
0–25	Ap	10YR 8/2	CAN	Angular blocky	Well drained	Loose	Common, coarse	Gently undulating & low flooding risk	Lowland: Bajada Plain (Downstream)
25–65	Bk	10YR 4/4	CAN, SAX	Massive		Slightly hard	Few, fine		
65–105	2Ck1	10YR 8/3	CAN	Subangular blocky		Slightly hard	Very few, fine		
105-145	2Ck2	10YR 7/6	None	Subangular blocky		Moderately hard	None		
SMU3: Moderately deep, coarse-textured, slightly saline, moderately calcareous soils with undulating topography.									
0–10	C	10YR 8/6	None	Single grain	Somewhat poorly drained	Slightly hard	Few, medium	Undulating & moderate to high flooding risk	Midland (Midstream)
10–33	Ck	10YR 8/4	CAC, CAN	Massive		Moderately hard	Very few, fine		
33–70	2Cm	10YR 8/3	MNF	Subangular blocky		Very hard	None		
70–95	Cr	10YR 8/8	None	Massive		Extremely hard	None		
SMU4: Shallow, coarse-textured, nonsaline, slightly calcareous, with undulating topography.									
0–17	C	10YR 8/4	None	Single grain	Poorly drained	Moderately hard	None	Undulating & very high-risk flooding	Upland (Upstream)
17–45	Cr	10YR 7/2	None	Massive		Very hard	None		

Explanations: Horizon master and suffix designations were made based on Soil Survey Staff (2022). 7.5YR 4/2, 4/4, 5/4 (brown), 7.5YR 4/6, 5/8 (strong brown), 10YR 3/1 (very dark gray), 10YR 5/4 (yellowish brown), 10YR 7/2 (light gray), 10YR 7/6, 7/8, 8/6, 8/8 (yellow), 10YR 8/2, 8/3, 8/4 (very pale brown); Pedogenic features: FDS: finely disseminated salts, SAX: salt crystals, CAM: carbonate masses, CAN: $CaCO_3$ nodules, CAC: carbonate concretions), CAF: carbonate coats; CLF: clay films; MNF: manganese films.

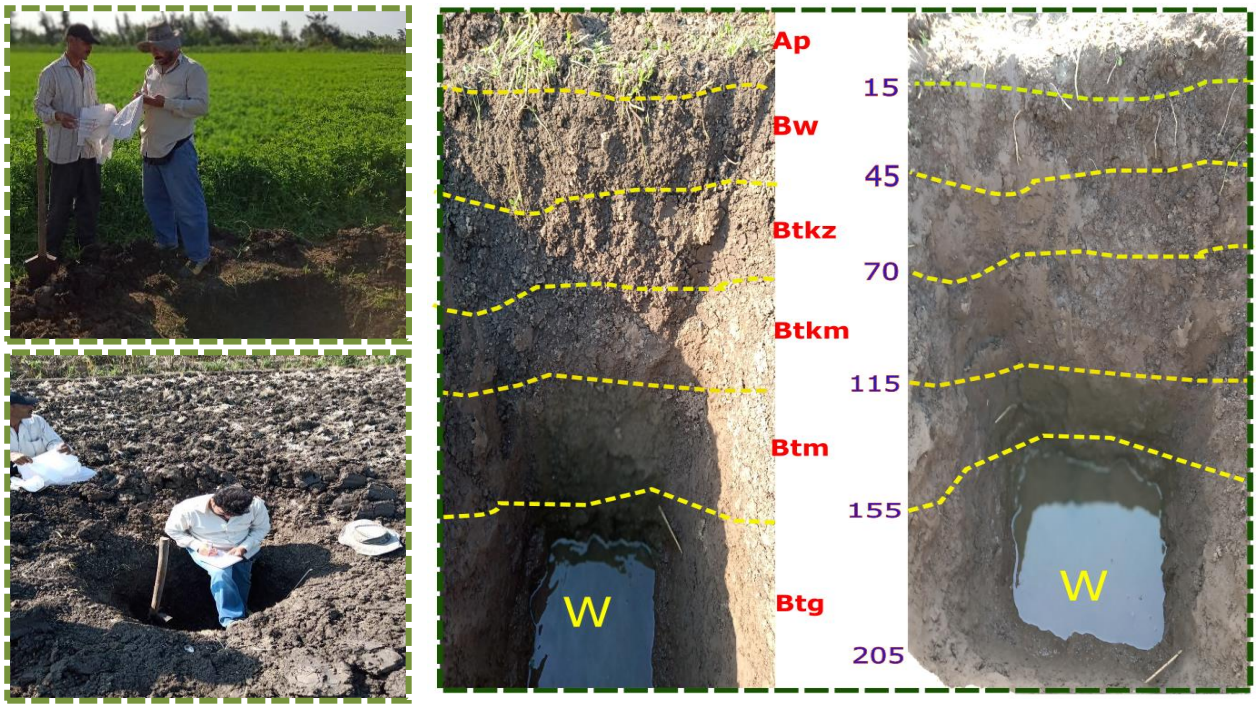

Fig. (13): Reference pedons of SMU1 limited by waterlogging (Root-limiting horizons/layers).

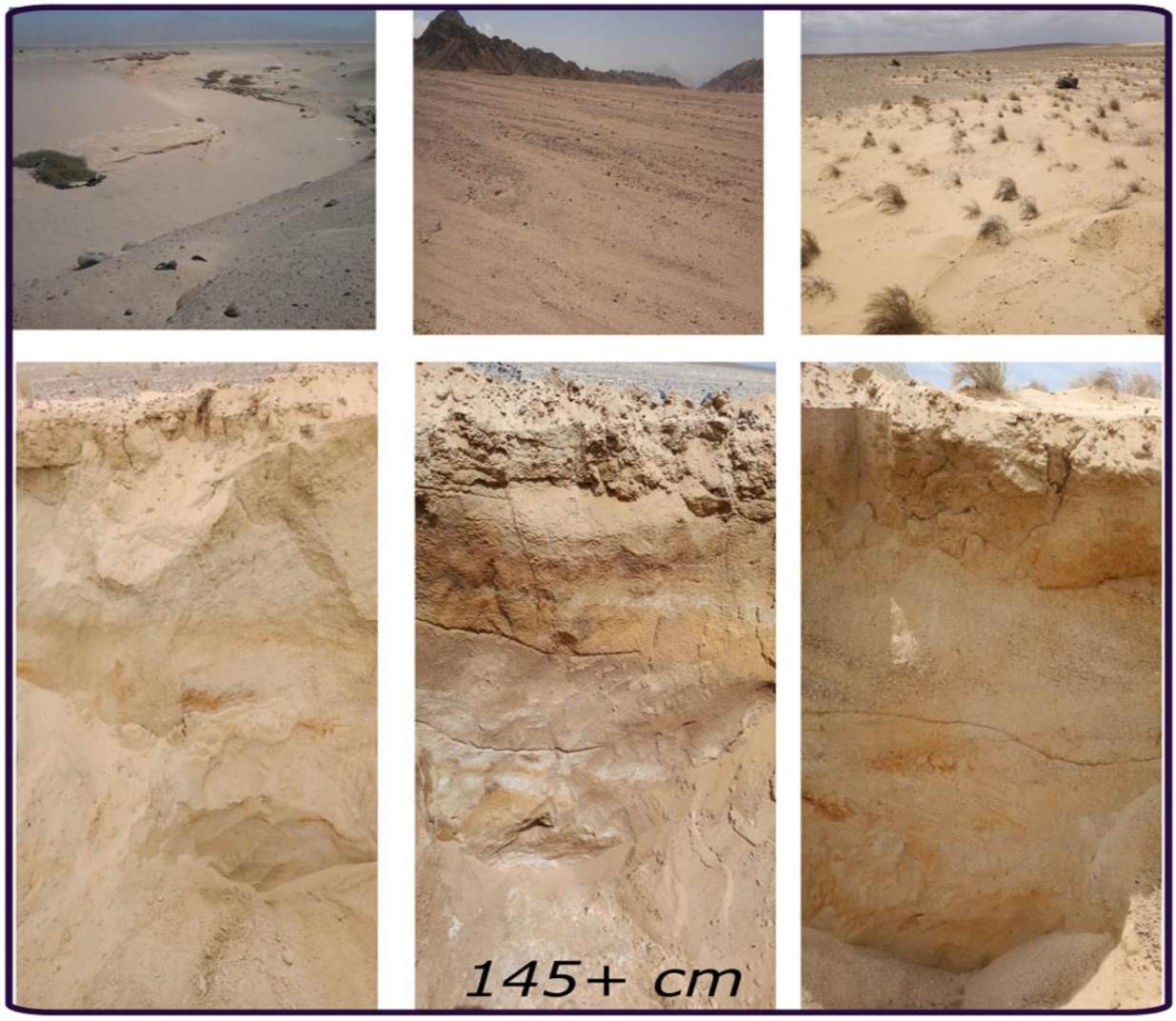

Fig. (14): Reference pedons of soil mapping 2 (SMU2) in the Wadi El-Madamude study area.

Table (2): Accurate soil physical characteristics of the soil profile at Wadi El-Madamude, East Luxor, Upper Egypt.

Horizon suffix	Horizon thickness(cm)	Coarse fragments(%)	Particle size analysis (%)			Textural class	Silt/Clay ratio	BD (g cm^{-3})	FC (%)	PWP (%)	AWHC (%)
			Sand	Silt	Clay						
SMU1: Deep, moderately fine textured, moderately saline, strongly calcareous soils with almost flat topography.											
Ap	15	3.25±0.65	52.49±3.23	26.45±1.42	21.06±1.35	SCL	1.26±0.56	1.10±0.38	37.5±2.56	19.7±1.00	17.80±0.89
Bw	30	1.36±0.09	43.75±2.71	26.90±1.33	29.35±1.65	CL	0.92±0.32	1.27±0.55	30.4±2.11	16.9±0.95	13.50±0.85
Btkz	25	14.25±0.84	28.80±2.01	30.15±1.54	41.05±2.99	C	0.73±0.23	1.53±0.98	31.4±2.22	17.2±0.98	14.20±0.66
Btkm	45	10.36±0.96	27.02±1.98	40.3±2.87	32.68±2.32	CL	1.23±0.47	1.69±0.79	35.7±2.01	20.4±1.05	15.30±0.76
Btm	40	9.65±0.19	50.35±3.15	27.64±1.68	22.01±1.23	SCL	1.26±0.56	1.43±0.35	34.8±2.02	19.2±0.99	15.60±0.79
Btg	50	3.65±0.07	23.30±1.05	55.01±3.45	21.69±1.18	SiL	2.54±0.87	1.39±0.28	34.0±2.01	17.6±0.96	16.40±0.83
W	The water table at 205 cm										
Weighted mean		**7.2**	**35.2**	**37.2**	**27.6**	**CL**	**1.45**	**1.44**	**33.9**	**18.5**	**15.4**
SMU2: Deep, moderately coarse textured, slightly saline, strongly calcareous soils with gently undulating topography.											
Ap	25	2.65±0.03	70.71±3.45	20.60±1.01	8.69±0.74	COSL	2.37±0.31	1.19±0.36	27.6±1.45	11.2±0.68	16.4±0.94
Bk	40	0.25±0.01	48.07±2.86	25.09±1.11	26.84±1.54	SCL	0.93±0.06	1.26±0.44	37.8±1.54	20.4±1.06	15.7±0.74
2Ck1	40	1.36±0.03	63.60±3.39	29.35±1.26	7.05±0.69	COSL	4.16±0.34	1.32±0.47	21.5±1.36	9.7±0.81	11.8±0.89
2Ck2	40	2.65±0.07	74.95±3.48	15.70±0.96	9.35±0.81	FSL	1.68±0.19	1.33±0.47	24.1±1.39	11.2±0.97	12.9±0.92
Weighted mean		**1.6**	**63.7**	**22.9**	**13.4**	**COSL**	**2.28**	**1.28**	**26.9**	**13.5**	**13.4**
SMU3: Moderately deep, coarse-textured, slightly saline, moderately calcareous soils with undulating topography.											
C	10	12.00±0.68	89.05±3.50	6.54±0.54	4.41±0.32	S	1.48±0.13	1.65±0.08	9.8±0.99	4.3±0.36	5.5±0.09
Ck	23	35.3±0.29	85.84±3.47	8.15±0.65	6.01±0.56	LCOS	1.36±0.11	1.57±0.07	19.7±1.10	8.7±0.74	10.0±0.92
2Cm	37	16.4±0.86	86.95±3.48	6.35±0.49	6.70±0.59	LCOS	0.95±0.08	1.59±0.04	20.3±1.23	9.1±0.83	9.4±0.82
Cr	25	14.3±0.75	87.39±3.49	9.15±0.76	3.46±0.12	COS	2.64±0.13	1.61±0.05	7.9±0.83	3.1±0.34	4.8±0.96
Weighted mean		**20.0**	**87.0**	**7.5**	**5.4**	**LCOS**	**1.55**	**1.60**	**15.8**	**7.9**	**7.9**
SMU4: Shallow, coarse-textured, nonsaline, slightly calcareous, with undulating topography.											
C	17	39.6±2.87	84.36±3.65	11.05±0.65	4.59±1.12	LCOS	2.41±0.16	1.54±0.06	16.4±0.84	7.9 ±0.62	8.5±0.65
Cr	28	41.1±2.96	91.03±4.15	3.31±0.25	5.66±1.65	COS	0.58±0.07	1.76±0.09	9.1±0.76	4.2±0.32	4.9±0.04
Weighted mean		**40.5**	**88.5**	**6.2**	**5.3**	COS	**1.27**	**1.68**	**11.9**	**5.6**	**6.3**

Explanation: BD (Bulk density); FC (Soil moisture content at field capacity); PWP (Permanent wilting point); AWHC (Available water holding capacity); C(Clay); SCL(Sandy clay loam); L (Loam); CL (Clay loam); SiL (Silty loam); COSL(Coarse sandy loam); FSL(fine sandy loam); S (Sand); LCOS (Loamy coarse sand); COS (Coarse sand). Each soil property's mean and standard deviation were statistically analyzed and calculated for each horizon/layer in the soil mapping unit. The weighted mean of the pedon is computed by multiplying the thickness of each horizon/layer by its property value, summing the results, and then dividing by the total depth of the soil pedon.

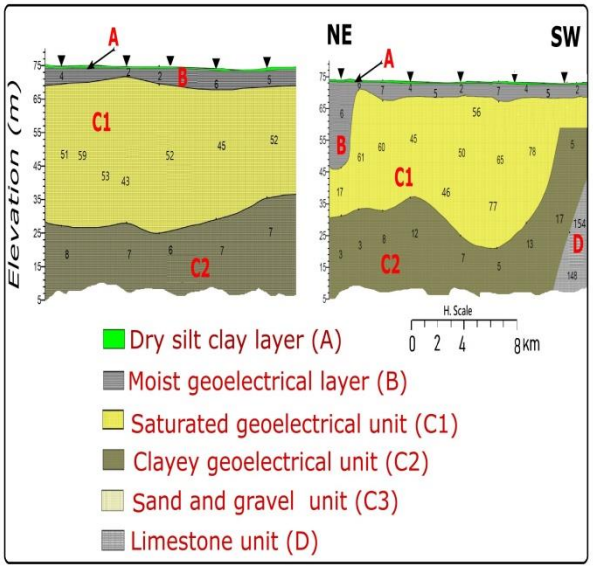

Fig. (15): Geoelectrical cross-sections within the Wadi El-Madamude study area (modified after Ismail et al., 2005).

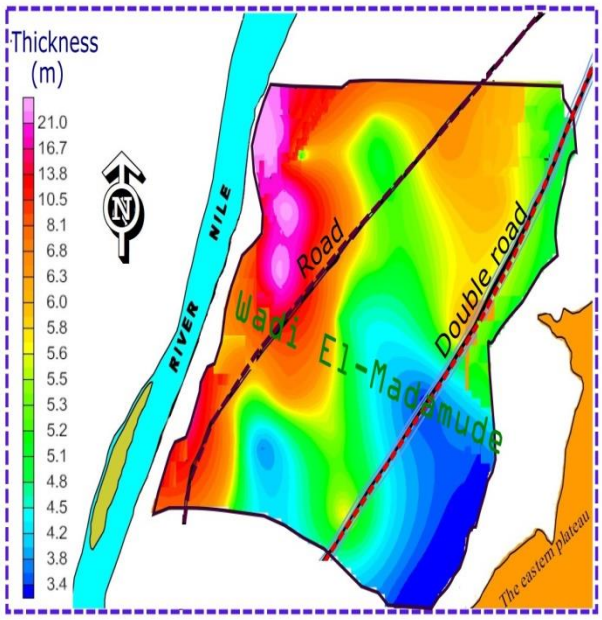

Fig. (16): Isopach map of the second geo-electric unit dry layer, Wadi El-Madamude (modified after Ismail et al., 2005).

Fig. 19 displays the findings of Youssef (2020) on Pleistocene aquifer groundwater in the Wadi El-Madamude lowland. The final resistivity model includes five geo-electric layers that accurately describe the subsurface geologic layering of the lowland at the investigated Wadi (Youssef, 2020). The layers consist of various lithologies, resistivities, depths, and thicknesses: surficial unconsolidated dry silts, consolidated sands and gravels, saturated sandstone, and clay intercalation (Plio-Pleistocene aquifer), clay with unsaturated sandstone and Checkley limestone. The elevation of Wadi El-Madamude's lowland is 110-160 meters above sea level (Fig. 19a). Fig. 19b shows a range of hydraulic conductivity values from 0.06 to 0.68 m/day. The hydraulic conductivities in the northern and central areas are below 0.5 m/day. The highest values are found in the study area's west-central, northeastern, and southern parts. In Fig. 19c, the transmissivity distribution reveals high places (>15 m^2/day) in south and western central lowlands and low areas (<8 m^2/day) in northwestern and central portions of the research area. The aquifer's modest hydraulic conductivities and transmissivities indicate a moderate production potential. Fig. 190d shows the salinity distribution map for Plio-Pleistocene aquifer water quality. Groundwater salinity typically falls to 500 ppm (Youssef, 2020). According to the investigation, salinity was lowest (<100 ppm) in the northwestern and east-central lowland areas. TDS studies indicate the Plio-Pleistocene groundwater aquifer is fresh (Iyasele et al., 2015).

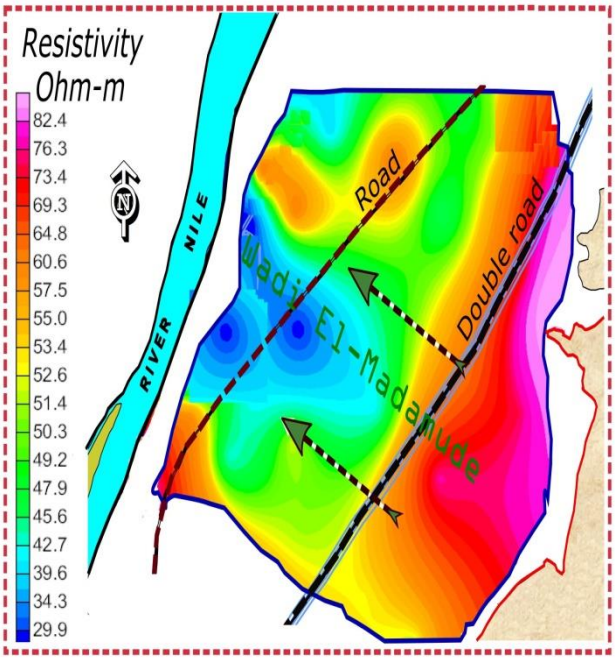

Fig. (17): True resistivity image of graded sand and gravel of the Quaternary aquifer in Wadi El-Madamude (modified after Ismail et al., 2005).

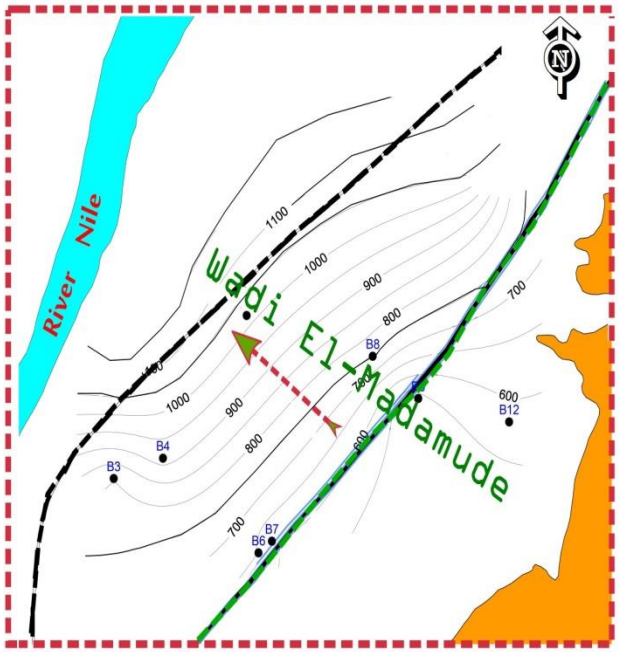

Fig. (18): Iso-salinity contour map of groundwater across Wadi El-Madamude (Ismail et al., 2005).

Land Potentiality Evaluation

The interpretative groups of the desert land evaluation technique (Q_LDLPE) were based on soil and water features (surface and groundwater) and socioeconomic and political collections, as shown in Table 6. As a result, the Q_LDLPE model classified the investigated lands into three potentiality classes (Fig. 20). SMU2 represents high potential areas on the Bajada Plain at lowland and covers an area of 45000 Faddan, accounting for 30% of the sample area. SMU1 and SMU3 represented moderate potential lands (57000 Faddan) on old Nile terraces landform and midland. Slightly potential lands (48000 Faddan) were found in the upland sections of the Wadi El-Madamude tributaries. The findings of the Red Sea agroecological zone conform with those findings of Elwan and Sivasamy (2013) in Indian sites, as well as Elwan and Khalifa (2014) in the Mediterranean region of Egypt, which emphasized the applicability of the Q_LDLPE model worldwide.

Despite the significant proportion of gravel in highland soils, crop output could not be regarded as severely limited. Furthermore, lesser depth and poor drainage were identified as severe restrictions to fruit production. As a result, upland was classified as having a low potential. In terms of non-soil criteria, severe flash floods, poor infrastructure (poor roads, irrigation facilities, and a lack of tools), inappropriate marketing (no access to markets, no competition, and weak incentives), the current land tenure system (plantations versus farming and competition among agriculture, mining, and other uses), and labor shortage were identified as significant constraints to increased agricultural production in the upland area. As a result, the Q_LDLPE model classified the upland areas as having a low potentiality. Under upland conditions, the small amount of prospective land is insufficient to cultivate crops profitably. Non-agricultural activities like road development are recommended in the upland area to connect the lower and top areas of the studied Wadi.

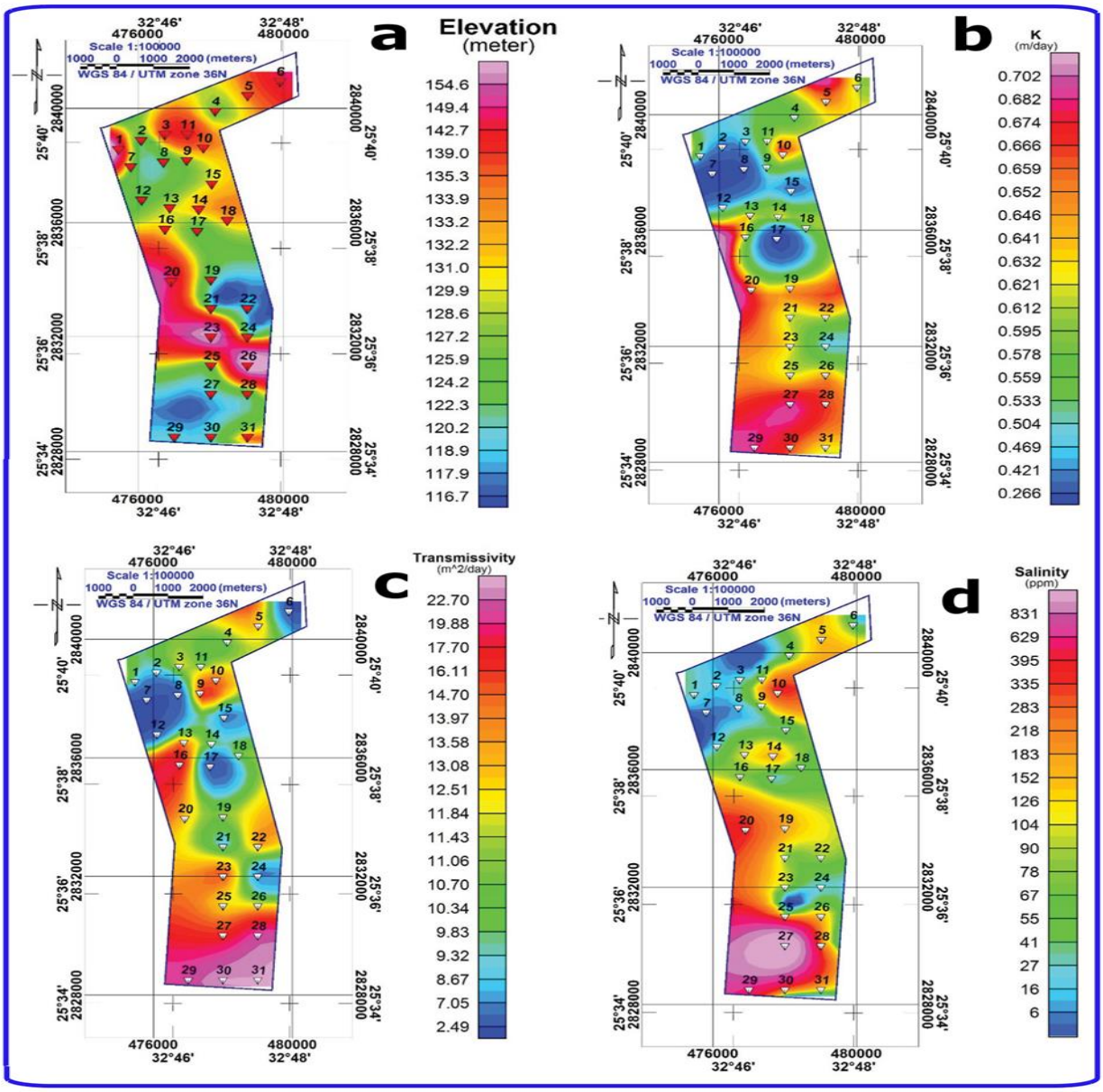

Fig. (19): Hydraulic parameters of Plio-Pleistocene aquifer of the study area. a) elevation model, b) hydraulic conductivity map, c) salinity map, and d) transmissivity map (after Youssef, 2020).

Table (3): Precise data on the chemical properties of the soils at Luxor's Wadi El-Madamude, Upper Egypt

Depth (cm)	Horizon suffix	pH	EC_e (dS/m)	$CaCO_3$ (%)	Gypsum (%)	ESP (%)	OC (%)	CEC cmol(+)/kg	Ca^{2+}/ Mg^{2+} Ratio
SMU1: Deep, moderately fine textured, moderately saline, strongly calcareous soils with almost flat topography.									
0–15	Ap	8.3±0.81	12.3±1.01	11.2±1.02	1.3±0.04	10.4±0.99	0.45±0.03	25.1±2.34	4.65±0.54
15–45	Bw	8.7±0.84	8.1±0.78	15.3±1.25	2.4±0.09	11.7±1.33	0.31±0.02	21.7±2.03	4.12±0.51
45–70	Btkz	9.1±0.89	15.2±1.23	25.4±1.98	0.9±0.01	16.5±1.26	0.37±0.03	31.2±2.58	2.94±0.32
70–115	Btkm	8.9±0.88	9.6±0.89	14.7±1.53	1.1±0.07	15.3±1.23	0.11±0.02	22.9±2.06	2.66±0.31
115–155	Btm	8.4±0.86	5.9±0.51	8.6±0.65	3.9±0.36	10.9±0.99	0.20±0.01	26.5±2.09	2.63±0.25
155-205	Btg	7.8±0.69	6.8±0.56	10.1±0.98	2.7±0.04	5.3±0.06	0.12±0.01	15.3±1.05	2.14±0.13
205+	W	Water table rising							
Weighted mean		**8.5**	**8.9**	**13.5**	**2.2**	**11.3**	**0.2**	**22.7**	**2.92**
SMU2: Deep, moderately coarse textured, slightly saline, strongly calcareous soils with gently undulating topography.									
0–25	Ap	7.9±0.71	4.3±0.36	13.4±1.46	0.1±0.03	10.7±0.99	0.39±0.04	12.9±1.03	2.63±0.36
25–65	Bk	8.2±0.74	2.9±0.19	10.3±0.99	0.5±0.06	11.2±1.01	0.27±0.03	27.1±2.01	2.61±0.34
65–105	2Ck1	8.6±0.79	3.6±0.24	26.5±1.97	0.4±0.5	12.7±1.03	0.13±0.02	11.5±1.00	3.23±0.45
105-145	2Ck2	8.3±0.76	5.8±0.43	19.9±1.05	0.9±0.6	11.1±1.02	0.07±0.01	13.7±1.01	2.45±0.29
Weighted mean		**8.3**	**4.1**	**18.0**	**0.5**	**11.5**	**0.2**	**16.7**	**2.74**
SMU3: Moderately deep, coarse-textured, slightly saline, moderately calcareous soils with undulating topography.									
0–10	C	7.8±0.68	3.7±0.62	5.3±0.45	1.1±0.98	3.7±0.06	0.19±0.02	5.4±0.29	0.93±0.07
10–33	Ck	8.4±0.87	3.5±0.57	13.4±1.01	0.5±0.36	12.2±0.89	0.13±0.01	6.9±0.37	0.81±0.05
33–70	2Cm	8.0±0.74	4.8±0.66	6.6±0.51	0.6±0.05	9.4±0.08	0.01±0.004	7.2±0.41	1.47±0.31
70–95	Cr	7.9±0.81	3.2±0.54	5.2±0.43	0.1±0.03	5.9±0.06	0.04±0.01	3.8±0.43	1.67±0.36
Weighted mean		**8.0**	**3.9**	**7.7**	**0.5**	**8.6**	**0.1**	**6.0**	**1.30**
SMU4: Shallow, coarse-textured, nonsaline, slightly calcareous, with undulating topography.									
0–17	C	8.1±0.79	0.3±0.06	1.3±0.04	0.4±0.05	9.7±0.98	0.11±0.02	6.1±0.55	1.45±0.21
17–45	Cr	7.6±0.63	0.1±0.03	1.9±0.06	3.6±0.11	6.1±0.54	0.02±0.01	4.7±0.36	1.63±0.29
Weighted mean		**7.8**	**0.2**	**1.7**	**2.4**	**7.5**	**0.1**	**5.2**	**1.56**

Explanations: Each soil property's mean and standard deviation were statistically analyzed for each horizon/layer in the soil mapping unit. The weighted mean of the pedon horizons is computed by multiplying the thickness of each horizon/layer by its property value, summing the results, and then dividing by the total depth of the pedon .

Table (4): Precise soil available nutrients for crop production at Wadi El-Madamude, East Luxor, Upper Egypt

Horizon suffix	Basal depth (cm)	Available macronutrients (mg kg^{-1})			Available micronutrients (mg kg^{-1})				
		AN	AP	AK	Iron (Fe)	Manganese (Mn)	Zinc (Zn)	Copper (Cu)	B (Boron)
SMU1: Deep, moderately fine textured, moderately saline, strongly calcareous soils with almost flat topography.									
Ap	15	29.1±2.35	15.2±1.31	145±5.21	3.91±0.62	1.30±0.32	1.02±0.09	0.45±0.03	0.02±0.01
Bw	45	27.6±2.32	8.3±0.74	115±4.98	4.16±0.82	1.44±0.38	0.93±0.08	0.32±0.02	0.01±0.01
Btkz	70	23.4±2.02	5.4±0.43	101±4.04	3.84±0.78	1.81±0.45	0.86±0.07	0.61±0.05	0.11±0.05
Btkm	115	15.0±1.02	3.6±0.29	120±4.85	4.67±0.87	1.76±0.42	0.64±0.055	0.43±0.03	0.08±0.06
Btm	155	13.6±1.01	6.2±0.37	134±5.04	5.28±0.92	1.63±0.39	0.55±0.04	0.25±0.02	0.07±0.02
Btg	205	24.2±2.04	2.6±0.14	95±4.08	5.35±0.97	1.18±0.43	0.28±0.02	0.19±0.01	0.03±0.01
W	205+								
Weighted mean		**20.9**	**5.6**	**115.4**	**4.72**	**1.52**	**0.63**	**0.34**	**0.05**
SMU2: Deep, moderately coarse textured, slightly saline, strongly calcareous soils with gently undulating topography.									
Ap	25	31.4±2.98	12.4±0.99	136±5.02	2.31±0.62	1.29±0.35	0.51±0.04	0.19±0.03	0.12±0.45
Bk	65	11.4±1.08	11.3±0.98	112±4.66	3.03±0.98	0.83±0.43	0.39±0.02	0.16±0.02	0.14±0.47
2Ck1	105	9.3±0.89	8.1±0.68	76±3.87	1.85±0.46	0.61±0.39	0.34±0.02	0.14±0.02	0.16±0.56
2Ck2	145	4.1±0.09	3.9±0.32	54±3.54	1.37±0.26	0.37±0.37	0.13±0.01	0.12±0.01	0.18±0.68
Weighted mean		**12.3**	**8.6**	**90.2**	**2.12**	**0.72**	**0.33**	**0.15**	**0.15**
SMU3: Moderately deep, coarse-textured, slightly saline, moderately calcareous soils with undulating topography.									
C	10	27.2±2.98	6.4±0.45	69±3.65	1.25±0.21	0.81±0.45	0.42±0.08	0.17±0.06	0.14±0.11
Ck	33	19.3±1.78	3.6±0.24	57±3.86	1.52±0.32	0.67±0.41	0.21±0.05	0.13±0.04	0.02±0.01
2Cm	70	14±1.09	4.2±0.35	43±2.86	1.76±0.39	0.43±0.39	0.14±0.04	0.09±0.04	0.04±0.01
Cr	95	5.4±0.03	1.2±0.087	20±1.57	1.94±0.41	0.26±0.33	0.13±0.06	0.08±0.03	0.03±0.01
Weighted mean		**14.4**	**3.5**	**43.1**	**1.70**	**0.48**	**0.18**	**0.11**	**0.04**
SMU4: Shallow, coarse-textured, nonsaline, slightly calcareous, with undulating topography.									
C	17	21.3±1.05	4.3±0.36	49±2.64	2.51±0.57	1.22±0.07	0.25±0.03	0.09±0.01	0.07±0.03
Cr	45	4.2±0.65	2.8±0.12	15±1.65	0.97±0.89	0.75±0.01	0.12±0.02	0.04±0.01	0.01±0.01
Weighted mean		**10.7**	**3.4**	**27.8**	**1.55**	**0.93**	**0.17**	**0.06**	**0.03**

Explanations: Each soil property's mean and standard deviation were calculated for each horizon/layer in the soil mapping unit. To determine the pedon's weighted mean, multiply the thickness of each horizon/layer by its property value, then aggregate the findings and divide by the total depth.

Table (5): Chemical properties of collected groundwater samples across the Wadi El-Madamude study area.

Well	Elevation (m, a.s.l.)	pH	EC_w (dS/m)	TDS (mg/l)	Soluble cations (ppm)				Soluble anions (ppm)			
					Ca^{2+}	Mg^{2+}	Na^{+}	K^{+}	CO_3^{--}	HCO_3^{-}	$SO4^{-2}$	Cl^{-}
1	157	7.50	0.78	499	113.5	35.6	89.7	3.2	Nil	39.3	109.4	109.3
2	151	7.41	1.08	691	132.3	33.2	150.0	5.2	Nil	35.5	198.5	137.3
3	137	7.33	0.57	366	105.0	35.6	55.5	1.7	Nil	34.1	69.3	65.2
4	139	7.65	0.90	576	105.6	36.3	145.3	6.2	Nil	46.3	147.5	89.7
5	121	6.78	0.87	559	89.3	35.3	159.3	6.4	Nil	22.2	59.4	188.3
6	121	7.22	1.60	1025	119.4	23.0	345.0	7.2	Nil	63.4	109.2	358.1
7	119	7.92	1.66	1060	111.3	29.4	419.3	7.5	Nil	48.2	99.7	345.1
8	115	7.81	1.79	1142	149.4	33.4	389.3	9.2	Nil	60.1	86.3	415.3
9	125	6.90	1.91	1219	154.5	41.1	400.0	8.4	Nil	55.4	95.3	465.0
10	107	7.22	1.78	1140	105.3	35.7	435.0	6.2	Nil	53.7	106.5	398.6
11	99	7.10	1.81	1157	133.7	51.5	399.4	11.5	Nil	49.4	111.5	401.2
12	109	7.01	1.85	1184	133.5	45.3	415.6	9.2	Nil	47.3	105.4	428.4
13	88	7.30	1.74	1112	117.3	45.4	405.1	12.4	Nil	40.2	105.1	387.2
14	87	7.60	2.41	1541	132.0	50.3	551.0	11.5	Nil	39.5	107.3	650.0
15	109	6.89	2.37	1518	145.4	53.3	580.7	12.5	Nil	50.1	117.4	559.3

Explanations: Calcium (Ca), Magnesium (Mg), Sodium (Na), Potassium (K), Carbonate (CO_3), Bicarbonate (HCO_3), Sulphate ($SO4^{-2}$), Chloride (Cl).

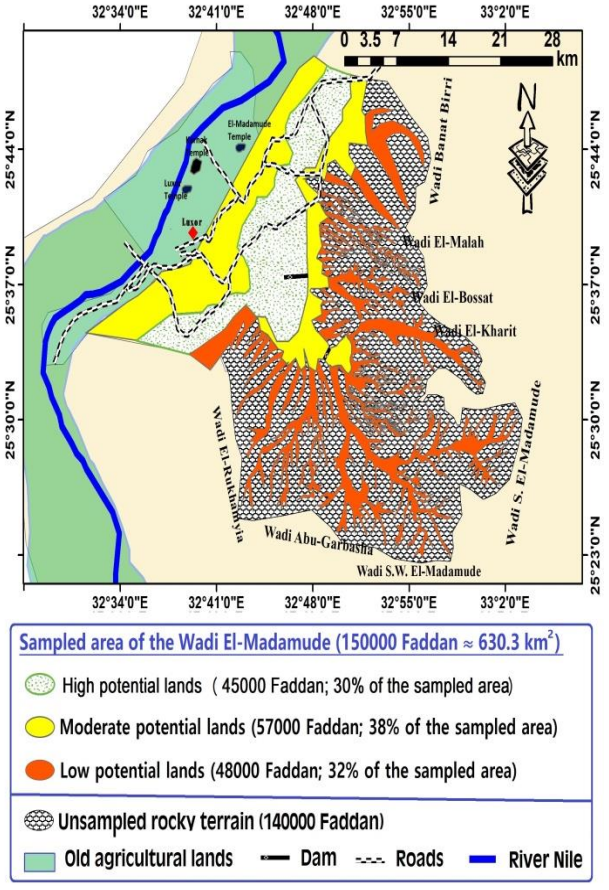

Fig. (20): Land potentiality classes of study area using Q_LDLPE method (1 Faddan≈4200 m²).

Q_LDLPE gave a moderate soil index for midland soils due to significant erosion danger, root-restrictive depth limitation at 95 cm, poor drainage, and coarse fragments. Due to flash floods, poor infrastructure, technical knowledge gaps, and weak institutional support, the land index ranged from 64-77% in the midland to 26-33% in the upland, indicating moderate and low potential, respectively, according to the Q_LDLPE model. The high potential land (index: 82-91%) in Bajada Plain is suitable for most crops in a profitable way under lowland conditions. Based on the optimum crop requirements and the characteristics offered by the studied lands, three land utilization types (LUTs) were determined and suggested by the Q_LDLAC model for agricultural development (Fig. 21; Table 7). The areas of Wadi tributaries were found to be unsuitable for the considered LUTs because of insufficient soil depth, high flooding hazard, severe erosion, and soil workability. These areas are located on upland and midstream, which could be used for non-agricultural activities.

The priority order for agrarian expansion was identified and advised for all crops based on the value-added for climate-smart crops. Fig. 21 depicts the prioritized land usage types (LUTs) for agricultural development in the research area. Based on their high market value as climate-smart crops, these crops were prioritized across the study area as optimum land usage types (LUTs) for successful cultivation. The priority order across the Wadi El-Madamude study area is as

follows: first priority for climate-smart fruits and crops (45000 Faddan) > second priority for salt-tolerant crops as organic greenhouse production (medicinal and aromatic plants) (39000 Faddan) > third priority for moderately deep-rooted crops as protected agriculture using precision farming management (18000 Faddan) > fourth priority for non-agricultural activity (48000 Faddan). The areas cultivated with first-priority innovative crops have high potentiality classes, while those for second and third-priority crops have moderate potentiality classes (Table 7).

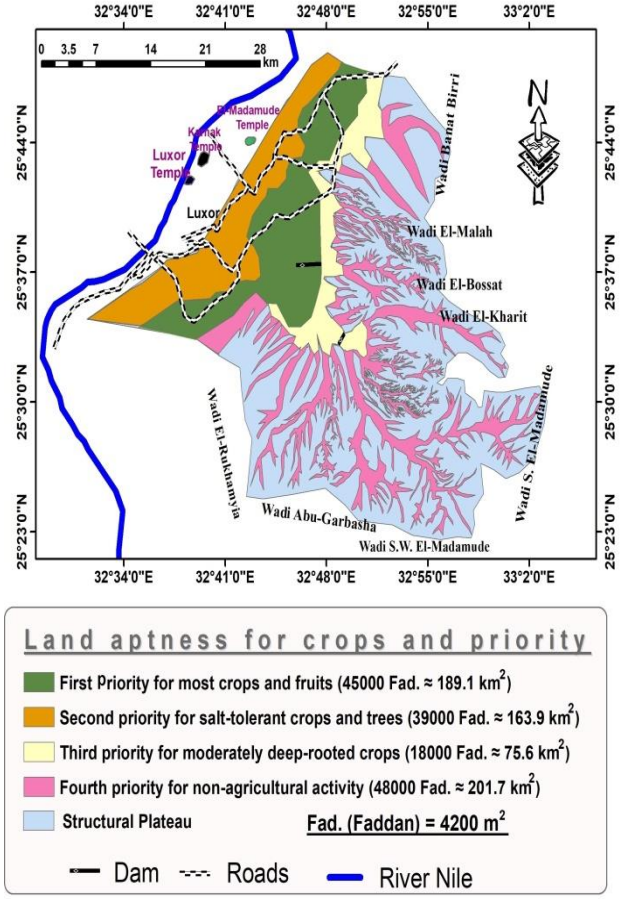

Fig. (21): Land priorities for climate-smart crops according to the Q_LDLAC land evaluation system.

The management guideline recommends precision farming using high-quality farmyard manure, mulching, compost, and bio-fertilizers to increase soil organic matter. Apply scientific technologies and soil, water, and crop management tools when cultivating indicated LUTs in the research region. Additionally, implementing environmental protection and water harvesting technology can reduce flash floods and erosion risks. Understanding existing technology and its latest advances is crucial to helping developing countries use rich crops for value-added goods.

Most restrictions on high-potential lands are modifiable criteria that might be addressed by introducing organic manures and leaching standards. Therefore, rather than other crops, this location is appropriate for the growth of fruit trees such as guava (*Psidium guajava*), olive (*Olea europaea*), and date (*Phoenix dactylifera*) (Fig. 21). Under the stress circumstances of these soils, the recommended products for SMU1 on historic Nile terraces have high appropriateness classes and are tolerant of soil salinity. As for the Red Sea ecosystem in Egypt, my findings agreed with those of earlier research conducted in comparable areas of India (Elwan, 2013) and the southwest Sinai of Egypt (Elwan et al., 2016). This research supports using a Q_LDLAC process as a customized method for evaluating desert resources.

The primary impediments to agricultural productivity in midland plain soils were high soil erosion, severe flash flooding, low fertility, salinity, and pH. It was recommended that agriculture be shielded from environmental dangers as a result. The area's intermediate potential land could only support relatively deep-rooted crops like squash, eggplant, carrot, cucumber, bean, peas, and pepper, as well as fragrant and medicinal plants like coriander, rose, mint, and senna. Farmers and stakeholders can cultivate cash crops on tiny plots through the protected cultivation of high-value vegetables and other horticultural crops in greenhouses in marginal and water-deficient areas where traditional cropping is not feasible. Using the Q_LDLAC technique, these crops were classified as having high aptness classes. Elwan et al. (2016) obtained similar results in Al-Tur, Sinai, Egypt soils. Furthermore, Elwan (2013) assessed field crops that are compatible with the local climate in the desert regions of Tamil Nadu, India, such as sesame (*Sesamum indicum*), cowpea (*Vigna unguiculata*), black gram (Vigna mungo), groundnut (*Arachis hypogaea*), maize (*Zea mays*), and sorghum (*Sorghum bicolor*).

DISCUSSION

Soil and water assessment are included in land potentiality evaluation (Elwan, 2019; Bhat et al., 2023). Accurate data on surface water and groundwater in the research area's Plio-Pleistocene and Quaternary aquifers were examined and updated for land evaluation and precision farming in Wadi El-Madamude. Soil characteristics, water resources and their quality, socioeconomic conditions, and political measures were all considered, as were land potentiality and crop appropriateness. Climate data were coupled with all other factors to determine various land utilization options and maximize crop production. These criteria in desert agricultural ecosystems necessitate significant amounts of precision agrarian data.

Furthermore, soil sensors, GPS, ArcGIS, and other geospatial technologies may be used in farms for smart and precision farming to collect cost-effective soil and groundwater irrigation information during agriculture, which is subsequently analyzed using big data analytics and saved in the ArcGIS method for monitoring all conditions in smart farming.

Understanding large amounts of data on irrigation water characteristics and soil parameters is crucial for agricultural sustainability and food security in the Wadi El-Madamude region. Farmers or investors can discover the ideal soil type for their crops by classifying land based on all correct historical criteria, including water and soil, thus improving soil health and maximizing crop productivity.

Salinity can reduce yields in susceptible vegetables. These veggies include beans, parsley, and salad greens. Winter break involves pouring water on bare soil to remove salt from sandy soils. This leaching process is more complicated in SMU1 clay soils. Most greenhouses lack drainage systems to remove excess water. The removal of essential nutrients through leaching may contaminate groundwater. Salt-tolerant crops retain salt in their biomass and actively diminish soil salinity. Salt-tolerant crops are useless at high soil salinity but can help sustain low salinity. Smart and digital agriculture is a management tool that focuses on all data number values for measurements, soil or water monitoring, and reactions to diverse variability in crops, fields, fertilizers, and fertility standards. It can assist in boosting crop yields as well as soil performance while lowering total input expenditures (Zhao et al., 2023). Only 30% of the agricultural lands in the trial area were highly prospective land based on Q_LDLPE for growing most crops and fruits, according to the aptness and suitability appraisal utilizing a Q_LDLAC approach and spatial overlays of all soil, water, and climate parameters. However, moderately potential lands may be used for two land utilization types (salt-tolerant crops and trees and moderately deep-rooted crops). Salt-tolerant crops such as oil crops (Canola, Jojoba, Jatropha, and Sesame) and food crops (Cassava, Quinoa, Triticale, Wheat, and Barley) may be grown on SMU1 soils (45000 Faddan). While moderately deep-rooted crops such as medicinal and aromatic plants (Rose, Coriander, Senna, Mint) are grown in the SMU3 (18000 Faddan), other crops such as cucumber, squash, eggplant, bean, carrot, peas, and chili pepper are also grown. Crops with a moderately deep root system are primarily rooted in the top 60-90 cm of soil. Potato crop cultivation prefers coarse-textured soils to prevent excessive moisture from rotting their tubers (Shrestha and Mahat, 2022). Among the investigated areas, 42% (SMU2 and SMU3) are highly suited for cultivating potatoes and are classified as high potential lands. Conversely, 39% with finer soils are marginally favorable and classified as moderately potential lands (Fig. 21).

Table (6): Potentiality classes at Wadi El-Madamude based on the Q_LDLPE method.

Item \ Potentiality class	High potential lands	Moderate potential lands	Low potential lands
Resultant index	82-91%	69-77%	26-33%
Landform & position	Bajada Plain (Lowland)	Midland and old Nile terraces	Upland
Area (Faddan)	45000	57000	48000
Limitations	**Low:** Slightly soil salinity, soil fertility,	**Moderate:** Soil salinity, calcareous, root-restrictive within the soil pedons, limited drainage	**High:** Erosion, shallowness, stoniness, flooding, soil fertility, poor drainage
Infrastructure	High	Moderate to high	Low
Irrigation water	Sufficient	Limited	Unknown
Tourism activities	High	High	High (recommended)

Table (7): Suggested climate-smart crops and their priority utilization for the Wadi El-Madamude study area.

SMU	Landform & area	Land potentiality (Q_LDLPE)	Suggested LUTs and their suitability (Q_LDLAC model)	Priority utilization
SMU2	Bajada Plain (45000 Faddan)	High potential lands	Suitable for most crops and trees such as food crops (quinoa, wheat, triticale, cassava, barley, maize), fruit trees (guava, pomegranate, olive, figs, and date palm), vegetables (tomatoes, cucumber, peppers, and squash); forages (Panicum virgatum, Bermudagrass, Perennial ryegrass).	**The first priority** for climate-smart crops, including fruits, food crops, vegetables, and forages as precision farming
SMU1	Old Nile terraces (39000 Faddan)	Moderate potential lands	Suitable for certain crops: Salt-tolerant crops and fruit trees Oil crops (Jatropha, Jojoba, Canola, Sesame).	**The second priority** for organic greenhouse production as climate-smart crops.
SMU3	Midland (18000 Faddan)	Moderate potential lands	Suitable for only moderately deep-rooted crops Some vegetables and medicinal and aromatic plants (Rose, Coriander, Senna, Mint)	**The third priority** for protected agriculture using precision farming management
SMU4	Upland (48000 Faddan)	Low potential lands	Unsuitable for cultivation	**The fourth priority** for non-agricultural activities, such as the construction of roads and dams for water harvesting

1 Faddan= 4200 m^2

Crops vary by land type and may not thrive in particular environments, even if they are better suited for other crops. Different soil types have different crop kinds; therefore, selecting the best produce for soil conditions is crucial. The Q_LDLAC technique uses accurate soil, water, and climate data from Wadi El-Madamude to predict the best yields for each soil mapping unit. Farmers and decision-makers can use these maps to choose crops for different soil types. For instance, decision-makers can choose agricultural areas for high-yield crops like vegetables or food crops (e.g., wheat or corn) and low-water-demand crops like potatoes or peppers. These crops help decision-makers maximize farm production and profitability while decreasing crop failure from improper soil type and growth circumstances. These maps can help farmers identify regions that need further soil treatment or fertilizer for intelligent farming. This farming technique enhances soil health and boosts crop yield. Farmers can maximize profits and decrease costs by choosing crops that thrive in appropriate soil types. Farmers can utilize the precise technique to calculate planting time, fertilizer use, and plant spacing for increased agricultural yield, as soil and water quality directly impact crop productivity. Q_LDLPE and Q_LDLAC approaches help farmers choose the optimum crop on suitable land by reducing risk factors. Finally, soil suitability maps help farmers promote sustainable agriculture and optimize resource utilization.

The integration of precision farming systems with Q_LDLPE and Q_LDLAC systems provides more precise data for crop production optimization. Combining reliable data on climate, soil and water quality, and market demand can estimate crop output and eventual profitability for the farmer or producer. Precision farming may recommend the optimum amounts of plant nutrients and bio-pesticides by advising the farm on which fertilizers and agrochemicals to employ and in what quantities. Modifications to these models can be recommended based on the local conditions of the farms to attain the highest yields with the fewest inputs. This study will help farmers, producers, and decision-makers make informed decisions regarding cultivating certain land and soil types. It will boost agricultural production efficiency, preserve soil and water quality, reduce expenses, and boost farm produce.

CONCLUSIONS AND RECOMMENDATIONS

Choosing the correct crop requires careful consideration of elements such as irrigation water availability (surface or groundwater), environmental hazards, socioeconomic and political concerns, soil characteristics, and climate change. Precision agriculture may be applied to provide crop suggestions based on the land's potentiality and the soil's compatibility. Q_LDLPE and Q_LDLAC techniques were used to increase performance and accuracy by considering the abovementioned factors.

Discovered shallow groundwater flow pathways east of Luxor to the River Nile raised the groundwater table in the Bajada Plain. The water table rise was accompanied by a considerable increase in groundwater salinity in the same flow channel. The high groundwater near the old Nile terraces may be due to flood irrigation in freshly reclaimed regions on the floodplain transition, several kilometers east of Luxor and a few meters above it. Data indicates salt deposition on historic Nile terraces in the Wadi El-Madamude delta is caused by capillary water movement from high salinity groundwater or connate water in thick silty clay units.

Four units of 150000 (630.3 km^2) Faddan were mapped over Wadi El-Madamude using soil and terrain features. QLDLPE techniques were used to categorize the land resources of the examined Wadi into three categories: high, moderate, and low potential. The QLDLAC technique was used to reassess these classifications for various agricultural land utilization patterns, considering soil type and meteorological data from the research location. In the studied area, 45000 Faddan was recommended for mostly field crops and fruit trees, 39000 for salt-tolerant crops, and 18000 for moderately deep-rooted crops. The rest of the sampled region was not included in agricultural development. Growing drought- and salt-tolerant crops is crucial for Egypt to address water shortages and salinity, especially as the country faces climate change impacts.

Explore groundwater, soil features, environmental hazards, socioeconomic, political, and climate factors to discover the best productive crops for the conditions. Two evaluation models (Q_LDLPE and Q_LDLAC) were used to help farmers and investors choose the most profitable crop, reduce crop selection errors, and increase agricultural productivity. They also predict yield depending on the farmer's crop selection.

Sustainable management in Wadi El-Madamude suggests covering the land with crops or plants for great returns with minimal inputs. It enhances soil fertility and reduces the need for fertilizers and pesticides, reducing contamination risk. Crop rotations, legume crop rotations, and no-till farming improve soil quality and fertility while preventing contamination. Precision farming can prevent pesticide overuse and contamination. Consider these proposals to avoid the deterioration of historic Nile terraces' lowlands, categorized into local and regional measures for conservation. Local approaches to reduce water-table levels include using climate-smart crops, lowering groundwater levels, creating capillary barriers, and lining irrigation canals to avoid surface water seepage. Additionally, regional measures include switching from flood to subsurface irrigation, implementing reliable drainage systems in agricultural lands, and dewatering old Nile terrace sites to improve soil properties and health in SMU1.

Precision farming can use spatial information on site-appropriateness from crop diversification, and intensification plans to increase land productivity. It can prevent crop damage and optimize output rates under favorable growth conditions. Precision farming can help farmers choose crops more effectively by suggesting crops on their land. Future research will integrate socioeconomic data that assess inputs and outputs for

each soil type to improve and test models on diverse experimental soil data. Furthermore, future evaluation tools will proposed and tested based on loss and gains. These approaches will be known as Quantitative Desert Land Aptness for Crops (Q_NDLAC) and Quantitative Desert Land Potentiality Evaluation (Q_NDLPE), and they can be used in a variety of agricultural industries across the world in order to achieve food security.

REFERENCES

Ahmed, A.A. (2009). Land Use Change and Deterioration of Pharaonic Monuments in Upper Egypt. Journal of Engineering Science, Assiut University, 37(1), 161 – 177.

Ahmed, A.A. and G.E. Fogg (2014). The Impact of Groundwater And Agricultural Expansion on The Archaeological Sites at Luxor, Egypt, Journal of African Earth Sciences, 95, 93–104.

Ahmed, A.A.; G.E. Fogg; and M.A. Gameh (2014). Water use at Luxor, Egypt: consumption analysis and future demand forecasting. Environ Earth, Sci., 72, 1041–1053.

Ahukaemere, C.; D. Osujieke; and B. Ndukwu (2017). Horizon differences in micronutrient contents of soils of the coastal plain sands in Imo state, Southeast Nigeria, micronutrient contents of pedons formed under coastal plain sands. Bulgar. J. Soil Sci., 2 (2), 112–122.

Akhter, R. and S.A. Sofi (2022). Precision agriculture using IoT data analytics and machine learning. Journal of King Saud University – Computer and Information Sciences, 34, 5602–5618.

Bhat, S.A.; I. Hussain; and N. Huang (2023). Soil suitability classification for crop selection in precision agriculture using GBRT-based hybrid DNN surrogate models. Ecological Informatics, 75, 102-109.

Central agency for public mobilization and Statistics of Egypt (2022). Egypt Statistical Yearbook**.** Issue No. 108. Ref. No. 71-01111.

Chapagain, R.; T.A. Remenyi; R.M.B. Harris; C.L. Mohammed; N., Huth; D. Wallach; E.E. Rezaei; and J.J. Ojeda (2022). Decomposing crop model uncertainty: a systematic review. Field Crops Res., 279, 108448.

Dinssa, B. and E.Elias (2021). Characterization and classification of soils of Bako Tibe District, West Shewa, Ethiopia. Heliyon 7, e08279.

Dupuis, C.; M.P. Aubry; E. Steurbaut; W.A. Berggren; K. Ouda; R. Magioncalda; B. S. Cramer; D.V. Kent; R.P. Speijer; and C. Heilmann-Clausen (2003). The Dababiya Quarry Section: lithostratigraphy, clay mineralogy, geochemistry, and paleontology, Micropaleontology, 49, 41–59.

Egyptian Meteorological Authority (2022). Climatic Atlas of Egypt, Cairo, Egypt.

EL Shamy, I. Z.; M. I. Gad; M. Shedid; Y.A. EL Kazzaz; and M.A. Ammar (2013). Flash flood estimation in Luxor area with emphases on Wadi El-madamud, south Egypt. Egyptian Journal of Geology, 57, 103-117.

El-Shater, A.; A.M. Mansour; M.R. Osman; AA Abd El Ghany; and A. Abd El-Samee (2021). Evolution and significance of clay minerals in the Esna Shale Formation at Dababiya area, Luxor, Egypt. Egyptian Journal of Petroleum 30, 9–16.

Elwan, A.A. (2013). Novel approaches of land evaluation using geospatial technologies for planning sustainable development of desert areas. Ph.D. (Ag) Thesis, Tamil Nadu Agric. Univ., Coimbatore, India

Elwan, A.A. (2019). Drylands, Biodiversity, Management, and Conservation. *LC ebook* Chapter No. 9: Proper Evaluation of Desert Ecosystem for Sustainable Development. *Environmental Research Advances.* Nova Science Publishers, Inc., New York.

Elwan, A.A. (2020). Integrated Land Use Planning in Wadi El-Amal, Aswan Governorate, Egypt. Journal of Soil & Water Sciences; Suez Canal University, 5 (1), 31-48

Elwan, A.A. and M.E.A. Khalifa (2014). Evaluation of agri-Limitations for sustainable development at the area between El-Dabaa and El-Alamain, Mediterranean Region, Egypt. Alex. J. Agric. Res., 59 (3), 157-168.

Elwan, A.A. and R. Sivasamy (2013). Novel approach of land evaluation for natural resource management of desert ecosystem. Agricultural Graduate Student Conference on Food Safety and Food Security. Madras Agric. J., 100, 156-164.

Elwan, A.A.; M.E.A. Khalifa; and T.M.H. Yossif (2016). Soil resources inventory and agricultural development priorities in Al-Tur area, South-western of Sinai, Egypt. Zagazig J. Agric. Res., 43 (3), 923-937

Fadhilla, S.; A. Kusumandari; Y. Lubis, A. Siregar; and L., Hakim (2022). Land capability analysis using LCLP software in the cangkringan micro watershed model. In: IOP Conference Series: Earth and Environmental Science. IOP Publishing.

FAO (1970). Physical and Chemical Methods of Soil and Water Analysis. Soils Bulletin. No. 10, FAO, Rome.

FAO (2006a). Guidelines for Soil Description. Food and Agriculture Organization of the United Nations.

FAO (2006b). Plant nutrition for food security. In: Food and Agriculture Organization of the United Nations, 16. Issue 1.

Hazelton, P. and B. Murphy (2016). Interpreting soil test results: what do all the Numbers mean? Eur. J. Soil Sci., 58 (5), 1219-1220.

Ismail, A.; NL. Anderson; and J.D. Rogers (2005). Hydrogeophysical Investigation at Luxor, Southern Egypt. J. Environ. Eng. Geophys., 10 (1), 35–49.

Iyasele J.U., J. David, and D.J. Idiata, (2015). Investigation of the Relationship between electrical conductivity and total Dissolved solids for Mono-Valent, Di-Valent, and TriValent Metal Compounds. Int J Eng Res Rev., 3(1), 40–48.

Kamel, E.R. (2004). Geology of Luxor Area and its Relationship to Groundwater Uprising under the Pharaohs Temples. M.Sc. Thesis, Aswan Faculty of Science, South Valley University, Egypt.

Kayode, O.T.; H.I. Okagbue; and J.A. Achuka (2018). Water quality assessment for groundwater around a municipal waste dump site. Data in Brief, 17, 579–587. https://doi.org/10.1016/j.dib.2018.01.072.

Lindsay, W.L.; and W.A. Norvell (1978). Development of a DTPA soil test for zinc, iron, manganese, and copper. Soil Sci. Soc. Am. J., 42, 421–428.

Lu, R.K. (2000). Analytical Methods of Agricultural Chemistry in Soil. China Agricultural Scientech Press, Beijing, China.

Mani, A.K., Santhi, R., and Sellamuthu, K.M., (2007). A Handbook of Laboratory Analysis. 1st edition. ISBN: 978-81-902558-8-2, AE Publications, Coimbatore, Tamil Nadu, India.

Mondal, T.K.; and S. Sarkar (2021). Irrigation intensity in North Twenty-Four Parganas district, West Bengal, India. Miscell. Geograph., 25 (4), 246–258.

Munsell Color (2009). Munsell Soil-Color Charts with Genuine Munsell Color Chips. 2009 Year Revised /2010 Production. Gretagmacbeth. New Windsor, NY. www.munsell.com

Naidu, L.G.K.; V. Ramamurthy; O. Challa; R. Hegde; and P. Krishnan (2006). Manual on Soil Site Suitability Criteria for Major Crops, National Bureau of Soil Survey and Land Use Planning, Nagpur.

Othman, A., I.M. Ibraheem, H. Ghazala, H. Mesbah, and T. Dahlin, (2019). Hydrogeophysical and hydrochemical characteristics of Pliocene groundwater aquifer at the area northwest El Sadat city, West Nile Delta, Egypt.

Rabeh, T.; B. Sayed; and A. Mohamed (2017). Integration of geophysical tools for delineating structures controlling the groundwater reservoirs at Baharia Oasis, Western Desert, Egypt. J. Geosci., https://doi.org/10.1007/s12303-016-072-3.

Reynolds, J.M., (2011). An Introduction to Applied and Environmental Geophysics, second ed. John Wiley & Sons.

Said, R. (1990). The geology of Egypt – Balkema, USA. The geology of Egypt, A. Balkema, Rotterdam, Netherland.

Salman, S.A.; M. Arauzob; and A.A. Elnazera (2019). Groundwater quality and vulnerability assessment in west Luxor Governorate, Egypt. Groundwater for Sustainable Development, 8, 271–280.

Schoeneberger, P.J.; D.A. Wysocki; E.C. Benham; and Soil Survey Staff (2012). Field book for describing and sampling soils, Version 3.0. Natural Resources Conservation Service, National Soil Survey Center, Lincoln, NE.

Shrestha, S. and J., Mahat (2022). Sustainable Food Security: How To Feed An Increasing Population? A Review. INWASCON Technology Magazine (i-TECH MAG) 4, 15–18.

Soil Science Division Staff (2017). Soil survey manual. United States Department of Agriculture (USDA), Agriculture Handbook No. 18. Natural Resources Conservation Service, Washington, DC.

Soil Survey Staff (2014). Kellogg Soil Survey Laboratory Methods Manual. Soil Survey Investigations Report No. 42, Version 5.0. R. Burt and Soil Survey Staff (Ed.), Lincoln NE: US Department of Agriculture, Natural Resources Conservation Service .

Soil Survey Staff (2022). Keys to Soil Taxonomy, 13th edition. USDA Natural Resources Conservation Service, Washington, DC.

Swaminathan, B.; S. Palani; and S. Vairavasundaram (2023). Feature fusion-based deep neural collaborative filtering model for fertilizer prediction. Expert Syst. Appl., 216, 119441.

Virk, A.L.; M.A. Noor; S. Fiaz; S. Hussain; H.A. Hussain; M. Rehman; M. Ahsan; and W. Ma (2020). Smart farming: an overview. Smart Village Technol.: Concep. Develop., 191–201.

Walter, A.; R.Finger; R.Huber; and N. Buchmann (2017). Smart farming is key to developing sustainable agriculture. Proc. Natl. Acad. Sci. 114 (24), 6148–6150.

Youssef, M.A.S. (2020) Geoelectrical analysis for evaluating the groundwater characteristics of Wadi El-Madamud Area, Southeast Luxor, Egypt, Journal of Taibah University for Science, 14:1, 1514-1526, DOI: 10.1080/16583655.2020.183 8776.

Zhao, J.; H. Xie; D. Liu; R. Huang; and H. Peng (2023). Climate-smart management for increasing crop yield and reducing greenhouse gas emissions in Beijing-Tianjin-Hebei, China. Agricultural and Forest Meteorology, 339, 109569.

الملخص العربي

تقييم الموارد الأرضية وإستكشاف المياه الجوفية من أجل الزراعة الدقيقة بوادي المدامود، شرق الأقصر، صعيد مصر

عادل عبدالحميد علوان خليل[1] و مصطفى سعيد مصطفى برسيم [2]

[1]قسم البيدولوچي، مركز بحوث الصحراء، 1ش متحف المطرية، رقم بريدي 11753، القاهرة، مصر

[2]قسم الاستكشاف الچيوفيزيائى، مركز بحوث الصحراء، 1ش متحف المطرية، رقم بريدي 11753، القاهرة، مصر

لتعزيز الإنتاج الزراعي، يجب على صناع القرار معرفة أنواع النباتات المثالية لأنواع الأراضي المختلفة استنادًا إلى المتغيرات المكانية للماء والتربة والبيئة والمُناخ. تم إجراء البحث على مساحة 150000 فدان (≈ 630,3 كم^2) في وادي المدامود شرق الأقصر بصعيد مصر؛ لتقييم الموارد المائية والأرضية بشكل صحيح لاختيار أفضل تركيب محصولي يتناسب مع نوع التربة وجودة مياه الري والمُناخ. وبناءً على ذلك، تم دمج نموذج التقييم الوصفي لقدرة الأراضي الصحراوية (Q_LDLPE) مع نظام تقييم ملائمة الأراضي الصحراوية لإنتاج المحاصيل (Q_LDLAC) . وتم تحديد أربعة أشكال أرضية في وادي المدامود، هي كالتالي: أراضي المصاطب النيلية القديمة Old Nile Terraces، وسهل الباجادا، Bajada Plain والمناطق متوسطة الارتفاع Midland والمناطق الجبلية المرتفعة Upland . وتم تقييم المياه الجوفية عبر وادي المدامود من خلال الدراسات الجيوفيزيائية. تعتمد منطقة بحث وادي المدامود على مياه نهر النيل السطحية وكذلك مصادر المياه الجوفية للري. يحتوي وادي المدامود على حوضي مياه جوفية، وهما: الحوض الجوفي الرباعي الضحل Shallow Quaternary Aquifer والحوض الجوفي البليوبليستوسين العميق Deeper Plio–Pleistocene Aquifer. أوضحت نتائج التحليل المعملي لعينات المياه، أن مياه نهر النيل تعتبر عالية الجودة في منطقة الدراسة بوادي المدامود بدرجة ملوحة تبلغ 175 ملليجرام/لتر. وكما وتتراوح ملوحة المياه الجوفية في وادي المدامود من 449 ملليجرام/لتر في الجزء الشرقي للوادي إلى 1518 ملليجرام/لتر في الجزء الغربي للوادي تحت الدراسة وبالقرب من النيل، والتي تعود إلى الحوض الجوفي الرباعي. كما اوضحت نتائج الدراسة، أن الملوحة وارتفاع مستوى المياه من أهم أسباب تدهور التربة في أراضي المصاطب النيلية القديمة Old Nile Terraces بسبب الأسلوب الخاطئ في الري بالمناطق المزروعة حيث إتباع الري بالغمر، ومن ثم تبخر المياه ذات الملوحة العالية نسبيًا تاركة الأملاح بنطاق قطاع التربة مسبباً أفق ملحي Salic Horizon، كما أن التسرب الرأسي لهذه المياه ادى إلى تدهور المياه الجوفية في الجهة الغربية للوادي بمنطقة المصاطب النيلية، هذا بالاضافة الى وجود الطبقة الحاملة للمياه شديدة التملح (Thick silty clay unit) والتي تنتمي للخزان الجوفي الرباعي والتي ساهمت بشكل كبير في زيادة عمليات التملح. تم رسم وتحديد أربعة وحدات خرائطية للأراضي Soil mapping units في وادي المدامود استنادًا إلى خصائص التربة والتضاريس. كما تم تصنيف وادي أراضي المدامود تحت الدراسة إلى ثلاث فئات طبقاً لمنهجيات Q_LDLPE وهي: أراضي عالية الإمكانيات (30%) High Potential Lands، ومعتدلة او متوسطة الإمكانيات الأرضية (38%) Moderate Potential Lands، وأراضي ذات إمكانيات منخفضة (32%) Low Potential Lands. تم تحديد وتوصية بأن يتم تحديد ترتيب الأولويات للتوسع الزراعي في وادي المدامود بناءً على القيمة المضافة من المحاصيل الذكية والتي لها القدرة على التكيف مع المناخ حيث تم تقييم هذه الفئات مرة أخرى لأنواع استخدامات الأراضي الزراعية المختلفة (LUTs) استنادًا إلى نوع التربة وجودة مصادر مياه الري مُتكاملاً مع البيانات المُناخية للمنطقة باستخدام تقنية نظام Q_LDLAC مع التوصية بزراعة معظم المحاصيل الحقلية وأشجار الفاكهة للأراضي عالية الإمكانات High Potential lands على مساحة 45000 فدان بسهل الباجادا Bajada Plain كأولوية أولى، بينما يوصى بزراعة المحاصيل التي تحتاج إلى كميات صغيرة من المياه في الأراضي ذات الإمكانيات المتوسطة Moderate Potential Lands كأولوية ثانية على مساحة 39000 فدان بمنطقة المصاطب النيلية ، بالاضافة إلى إستخدام اراضي Midland في زراعة بعض الخضروات والنباتات الطبية والعطرية كأولوية ثالثة على مساحة 18000 فدان ، مع إستبعاد الأراضي منخفضة القدرة الانتاجية Low Potential Lands من التنمية الزراعية والتي تشغل مساحة 48000 فدان مع إستخدامها لأغراض غير زراعية. ويجب إتخاذ معايير الحماية لمنع تدهور التربة ومياه الري بالأراضي المنخفضة بالمصاطب النيلية، حيث زراعة المحاصيل التي تستهلك أقل كمية من الماء والتي تتوافق مع ظروف التغيرات المناخية بالمنطقة، علاوة على خفض مستوى المياه الجوفية باستخدام آبار التجفيف أو الصرف الجوفي، وتركيب حواجز زجاجية، وتبطين القنوات الزراعية لمنع تسرب المياه إلى الطبقات

السطحية. وبالإضافة إلى ذلك، إتباع أنظمة الري الحديث وخاصة الري تحت السطحي، واستخدام نظام صرف جيد في الأراضي الزراعية بنظام الزراعة الدقيقة.. حيث يوصى بإتباع النهج الزراعي الدقيق Precision farming لأنه يزيد من إنتاجية الأراضي عن طريق استخدام المعلومات المكانية لبيانات التربة، المياه، المحصول ، والبيئة. كما يمكن لنظام الزراعة الدقيقة أن يمنع تلف المحاصيل عند حدوث ظروف غير مواتية ويحسن معدلات إخراج المحصول عندما تكون الظروف المناسبة للنمو موجودة. كما أنه قد يجعل النظام الزراعي الدقيق المزارعين يتخذون اختيارات أكثر معرفة بخصوص الزراعات التي يجب زراعتها في أراضيهم. وفي المستقبل القريب يجب استخدام البيانات الاقتصادية كمدخلات ومخرجات لتحديد الارباح المتوقعة بصورة أكثر دقة في ظل بيانات التربة والمياه لتحسين نماذج تقييم الأراضي الصحراوية بصورة كمية واقتصادية Economic and Quantitative، والتي يقترح تسميتها "بالنظم الكمية لتقييم أراضي الصحراء لزراعة المحاصيل " (Q_NDLAC)و "تقييم الإمكانات الكمية لأراضي الصحراء "(Q_NDLPE) والتي يمكن استخدامهما بشكل متنوع عبر جميع أنحاء العالم. مع إمكانية دمجها مع المنهجيات الوصفية لتقييم الأراضي والتي أستخدمت في هذه الدراسة من أجل إعداد قاعدة بيانات متكاملة عن كافة الموارد الطبيعية بكافة الخيارات مدعومة بالأرقام المتعلقة بالتكاليف والأرباح للمساهمة بشكل مُستدام في سد الفجو الغذائية تحقيقاً للأمن الغذائي.